Article

Cell Metabolism

β Cell Aging Markers Have Heterogeneous Distribution and Are Induced by Insulin Resistance

Graphical Abstract

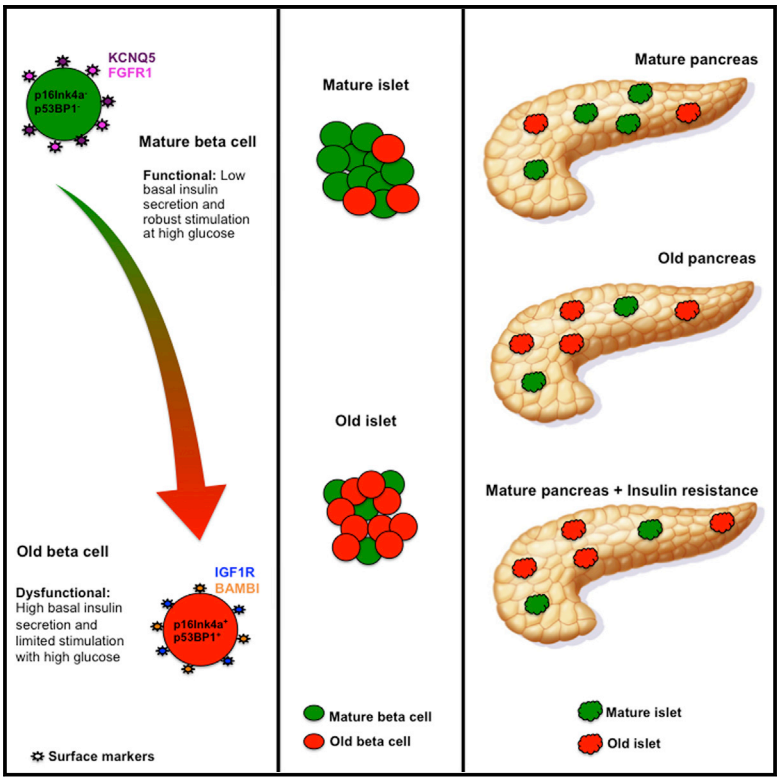

Highlights

- Subpopulations of pancreatic β cells differ and change proportions with aging
- Markers of β cell age show heterogeneity both within islets and between islets
- IGF1R-expressing β cells are senescent and have dysfunctional insulin secretion
- Insulin resistance accelerated expression of $p16^{Ink4a}$ and aging markers in β cells

Authors

Cristina Aguayo-Mazzucato, Mark van Haaren, Magdalena Mruk, ..., Jan Van Deursen, Gordon C. Weir, Susan Bonner-Weir

Correspondence

susan.bonner-weir@joslin.harvard.edu

In Brief

Aguayo-Mazzucato et al. show that the heterogeneity of pancreatic β cells is likely due to individual β cells at their respective life cycle stage expressing different markers and functional characteristics. Both age and environmental factors, including metabolic stress, can shift the composition of the β cell population contributing to diabetes.

Aguayo-Mazzucato et al., 2017, Cell Metabolism *25*, 898–910
April 4, 2017
http://dx.doi.org/10.1016/j.cmet.2017.03.015

CellPress

Cell Metabolism
Article

β Cell Aging Markers Have Heterogeneous Distribution and Are Induced by Insulin Resistance

Cristina Aguayo-Mazzucato,[1] Mark van Haaren,[1] Magdalena Mruk,[1] Terence B. Lee, Jr.,[1] Caitlin Crawford,[1] Jennifer Hollister-Lock,[1] Brooke A. Sullivan,[1] James W. Johnson,[1] Aref Ebrahimi,[1] Jonathan M. Dreyfuss,[1,2] Jan Van Deursen,[3] Gordon C. Weir,[1] and Susan Bonner-Weir[1,4,*]

[1]Joslin Diabetes Center, Harvard Medical School, One Joslin Place, Boston, MA 02215, USA
[2]Department of Biomedical Engineering, Boston University, Boston, MA 02115, USA
[3]Department of Biochemistry and Molecular Biology, Mayo Clinic, Rochester, MN 55905, USA
[4]Lead Contact
*Correspondence: susan.bonner-weir@joslin.harvard.edu
http://dx.doi.org/10.1016/j.cmet.2017.03.015

SUMMARY

We hypothesized that the known heterogeneity of pancreatic β cells was due to subpopulations of β cells at different stages of their life cycle with different functional capacities and that further changes occur with metabolic stress and aging. We identified new markers of aging in β cells, including IGF1R. In β cells IGF1R expression correlated with age, dysfunction, and expression of known age markers $p16^{ink4a}$, p53BP1, and senescence-associated β-galactosidase. The new markers showed striking heterogeneity both within and between islets in both mouse and human pancreas. Acute induction of insulin resistance with an insulin receptor antagonist or chronic ER stress resulted in increased expression of aging markers, providing insight into how metabolic stress might accelerate dysfunction and decline of β cells. These novel findings about β cell and islet heterogeneity, and how they change with age, open up an entirely new set of questions about the pathogenesis of type 2 diabetes.

INTRODUCTION

Reduced β cell mass and function are fundamental to the pathogenesis of type 2 diabetes (T2D) (Weir and Bonner-Weir, 2013). The loss of β cell mass is poorly understood, but the demands of insulin resistance are presumed to contribute to an accelerated loss of β cells. β cell function as determined by insulin secretion is also markedly impaired in T2D; this dysfunction is thought to result from β cells being in a diabetic environment, and strong evidence indicates that increased plasma glucose levels themselves result in major secretory abnormalities, hence the use of the term glucotoxicity. Type 2 diabetes (T2D) increases with age, with the majority of patients being above the fifth decade of life (Koopman et al., 2005).

Proposed mechanisms responsible for the loss of β cells in T2D include amyloid formation (Westermark and Westermark, 2013) and endoplasmic reticulum stress (Kaufman, 2011), but their relative contributions are not known. The pathology of the islets in T2D (Gepts and Lecompte, 1981) seems to provide major clues that should lead to novel ways to examine the problem. For instance, islets in T2D are strikingly heterogeneous: many look completely normal, some contain large deposits of amyloid and others none. To understand how the pathology reached that point, it seems important to understand islet and β cell heterogeneity and how they change with aging.

It has been known for years that there is considerable β cell heterogeneity, which has been mostly characterized by differences in secretion (Pipeleers et al., 1994). A variety of different parameters that vary among β cells have been examined in rodents: secretory function (Salomon and Meda, 1986), insulin expression (Katsuta et al., 2012), and telomere length (Guo et al., 2011; Peng et al., 2009). The concept of functional heterogeneity among β cells is bolstered by findings that they differ in sensitivity to glucose (Van Schravendijk et al., 1992) and can be recruited by higher glucose levels into both active biosynthetic (Bosco and Meda, 1991; Kiekens et al., 1992; Schuit et al., 1988) and secretory states when there is demand for more insulin secretion (Hiriart and Ramirez-Medeles, 1991; Hiriart et al., 1995; Karaca et al., 2009; Ling et al., 2006; Pipeleers, 1992).

New insights into heterogeneity have emerged with the recent report of four subtypes of human β cells defined by cell surface markers that are proportionally altered in T2D (Dorrell et al., 2016). One subtype found more often in T2D had higher basal insulin release and less response to glucose stimulation. Also, specialized hub cells, identified as 1%–10% of β cells with more active mitochondria and less insulin, have been recently reported to synchronize β cell oscillations (Johnston et al., 2016).

We hypothesized that β cells at each life stage have different markers and functional characteristics and that both age and environmental factors can shift the composition of the β cell population contributing to T2D development (Weir and Bonner-Weir, 2013). There is some understanding of the maturation of newly born β cells and some markers of old ("senescent") β cells. However, relatively little is known about the aging of β cells and how this influences cellular function and the rate of cell death. Cellular senescence, the phenomenon by which cells cease to divide and remain metabolically active, occurs

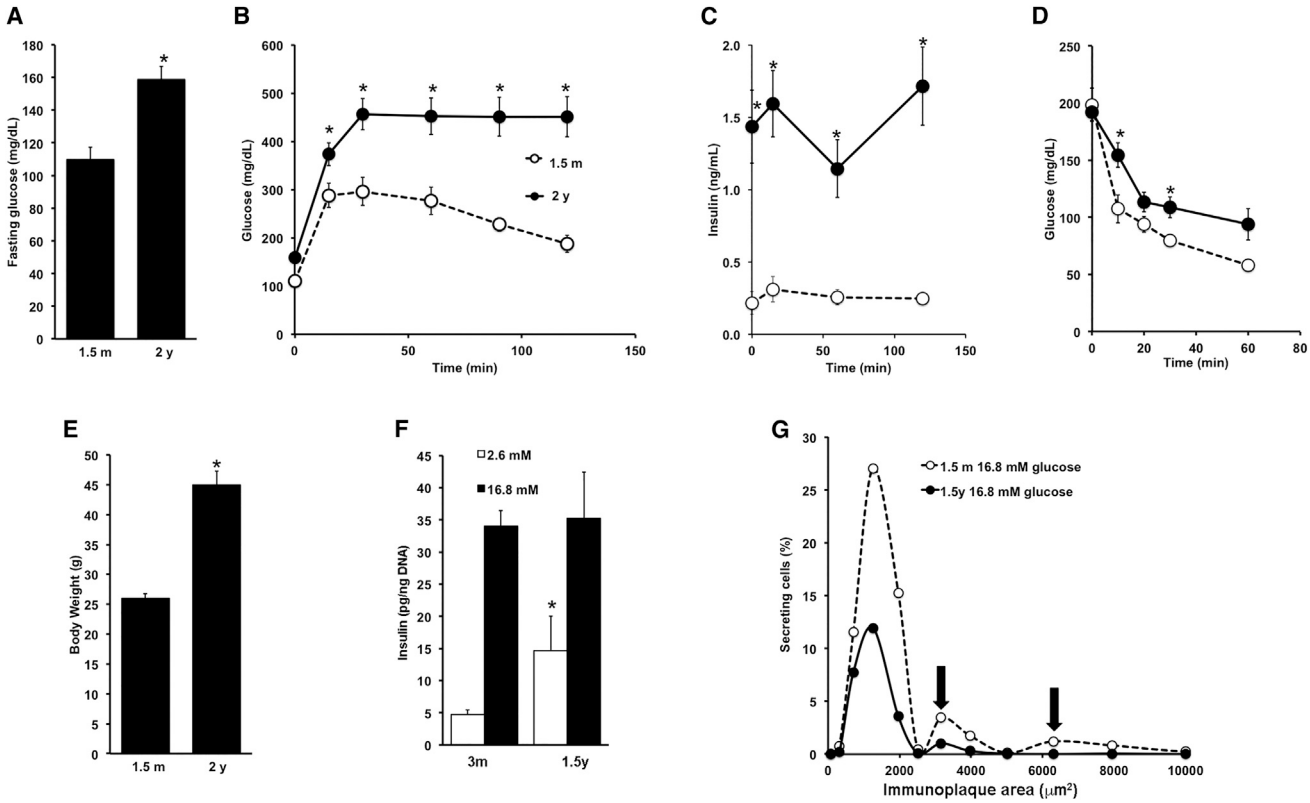

Figure 1. Development of Insulin Resistance, Loss of Glucose Tolerance, and Changes of Insulin Secretion as C57BL/6J Mice Age

(A–E) Elevation of fasting blood glucose (A), glucose intolerance (B), hyperinsulinemia (C), peripheral insulin resistance as determined by an insulin tolerance test (D), and weight gain (E) were observed in 2-year-old mice compared to 1.5-month-old mice. n = 6 for 1.5 months; n = 11 for 2 years; *p < 0.05 when compared to 1.5-month-old mice.

(F) By static incubation, glucose stimulated insulin secretion (GSIS) increased with age. n = 3 independent experiments in triplicate, *p < 0.01 when compared to 12-week-old mice.

(G) By RHPA, aged mice had decreased proportion of cells secreting at high glucose, particularly those secreting medium and large plaques (arrows). n = 495–1,008 cells counted/condition, 600–700 fields/condition from two independent experiments.

Mean ± SEM. Table 1 shows the aggregate data and the applicable statistics.

in response to different forms of stress and aging (Campisi and d'Adda di Fagagna, 2007). A known marker of senescence is *p16*^{Ink4a}, a cyclin-dependent kinase inhibitor encoded by the *Cdkn2a* locus. In β cells, its level of expression correlated with increased age and decreased proliferation (Krishnamurthy et al., 2006, 2004) and yet the marked cells were heterogeneously distributed in adult mouse and human islets (Chen et al., 2009; Dhawan et al., 2009; Köhler et al., 2011; Tschen et al., 2009).

Ways to identify new, young, middle-aged, old, and premorbid β cells on tissue sections and with flow cytometry should greatly enhance our understanding of β cells in the pathogenesis of diabetes. In this study we identified and validated markers of β cell aging and found marked heterogeneity of both islets and β cells that correlated with age-related functional decline. Moreover, increased secretory demand induced by insulin resistance led to the appearance of aging markers in β cells accompanied by functional changes. These novel findings about β cell and islet heterogeneity, and how they change with age, open up an entirely new set of questions about the pathogenesis of T2D.

RESULTS

β Cell Dysfunction during Normal Aging in Mice

Aging of C57BL/6J mice is accompanied by increased fasting glucose and worsening glucose tolerance (Figures 1A and 1B) as well as increased peripheral insulin resistance as reflected by hyperinsulinemia (Figure 1C), decreased glucose clearance during an insulin tolerance test (Figure 1D), and increased body weight (Figure 1E). Our data are consistent with that previously published showing these mice, carriers of the *Nnt* mutation, have glucose intolerance and reduced insulin secretion as early as 6 months of age (Freeman et al., 2006) (www.jax.org).

To evaluate the functional changes that accompany aging and insulin resistance in C57BL/6J mice, we assessed both static glucose-stimulated insulin secretion (GSIS) of isolated islets and the secretion of individual β cells with reverse hemolytic plaque assay (RHPA). Compared to islets from 3-month-old mice, islets from 1.4-year-old mice had increased insulin secretion at 2.6 mM glucose but no further increase at 16.8 mM (Figure 1F). A similar age-related increase in basal

Table 1. RHPA Secretion Summary from β Cells Obtained from Different Aged C57BL/6 Mice

	2.6 mM Glucose			16.8 mM Glucose		
	Area (μm^2)	Secreting Cells (%)	Secretion Index (Area × %)	Area (μm^2)	Secreting Cells (%)	Secretion Index (Area × %)
1.5 Months	1,246 ± 30[b]	26 ± 8[b]	312 ± 8[b]	1,704 ± 45	63 ± 1	1,074 ± 29
1.5 Years	1,712 ± 42[a,b]	30 ± 3	513 ± 12[a,b]	1,246 ± 31[a]	26 ± 4[a]	312 ± 8[a]

n = 495–1008 cells counted/condition, from 600–700 fields/condition, from two independent experiments.
[a]$p < 0.0001$ with respect to 1.5 months.
[b]$p < 0.0001$ with respect to 16.8 mM glucose.

insulin secretion was observed using INK-ATTAC mice, which do not develop glucose intolerance with age (Figures S1A–S1C). With RHPA, the immunoplaque area is directly proportional to the amount of insulin secreted by that cell (Salomon and Meda, 1986) (Figures S2A–S2D). Using dispersed islets from 1.5-month and 1.5-year mice, β cells from young mice increased their insulin secretion in response to 16.8 mM glucose 5.5-fold, as reflected by the secretion index (SI) as well as recruitment of non-secreting β cells at 2.6 mM glucose (where only 26% secrete insulin) to 63% secreting cells at 16.8 mM glucose. With age, β cell recruitment from 2.6 mM to 16.8 mM glucose was lost, and cells secreted more insulin at low glucose concentration with no further increase at high glucose (Table 1). In a cumulative frequency graph (Figure 1G) in which the average secretion (immunoplaque area) and the percentage of secreting cells at 16.8 mM glucose are plotted, it can be seen, as previously described (Aguayo-Mazzucato et al., 2011, 2006), that β cell function is heterogeneous with several functional subpopulations that secrete varying amounts of insulin in response to a given stimulus. Interestingly, with aging (1.5 years) these subpopulations changed, with many fewer β cells responsive to glucose (Figure 1G; Table 1).

β Cell Heterogeneity as Mice Age

Using C57BL/6J MIP:GFP mice in which GFP expression is driven by the insulin promoter, we previously reported changing populations of β cells from perinatal to 7 months of age based on GFP brightness, cell size, and granularity (Katsuta et al., 2012). Three subpopulations of pancreatic cells were identified and sorted according to GFP fluorescence levels. The proportions of these subpopulations changed markedly with age: the GFP^{low} subpopulation was large in young animals and decreased greatly by 4 months, whereas the GFP^{high} subpopulation was very small in the youngest mice and markedly increased by 4 months (Figure 2A). These results suggest that GFP^{low} cells may represent a younger, more newly formed β cell subpopulation while the GFP^{medium} and GFP^{high} subpopulations were older and consisted of both mature and senescent cells. To assess this, we sorted GFP+ β cells from young (embryonic day 15.5 [E15.5]–5 weeks), 2.5- to 7.5-month-old, and 1- to 2-year-old MIP:GFP mice for gene expression by qPCR. Expression of the β cell senescence marker *Cdkn2a* (*$p16^{Ink4a}$*) mRNA was not detected in any population of the young animals but increased with age in the GFP^{high} and GFP^{medium} subpopulations (Figure 2B); only at 1–2 years was it detectable in the GFP^{low} population. These data suggest simultaneous existence of differently aged subpopulations.

Age-Dependent Changes in β Cell Gene Expression Represent Both a Maturation and an Aging Process

We performed Affymetrix microarrays (n = 3–4 per age) on RNA from FACS-purified MIP:GFP β cells from different aged mice: (1) 3.5–9 week young; (2) 1 year old; (3) 2 years old. Analysis revealed age-related differential gene expression, with the greatest changes in expressed probe sets between young and 1 year old ($p < 0.05$) but with further changes between 1 and 2 years (Figure 2C; Figure S3). These changes show both the processes of maturation (less than 9 weeks old versus older) and of aging (1 year versus 2 years). The expression of *$p16^{Ink4a}$* and the senescent signature genes in β cells from aged MIP-GFP mice support our expectation that islets from older mice are enriched with senescent β cells.

Identification of Cell Surface Markers of Aged β Cells

Surface markers that allow identification and isolation of aged β cells could be a powerful tool to study the different β cell populations. Mining our microarray data for differential expression of plasma membrane genes (Figure 2D and Table S1), we selected potential markers of β cell age for evaluation, including *Kcnq5* and *Fgfr1*, which seemed higher in young mice, and *Igf1r*, *CD99*, and *Bambi*, higher in old mice (p value and FDR < 0.05). Similar to what we found for *$p16^{Ink4a}$* mRNA (Figure 2B), *Igf1r* mRNA levels were increased in the GFP^{high} and GFP^{medium} subpopulations of β cells from oldest animals compared to those of younger (Figure 2E). To validate these candidate genes as aging markers, we measured their expression in independent samples of islets using expression of *$p16^{Ink4a}$* as a benchmark for aging. With increasing age, *$p16^{ink4a}$*, *Igf1r*, and *Bambi* mRNA increased, whereas *Kcnq5* and *Fgfr1* decreased and *CD99* was unchanged (Figure 2F; Figure S4). Taken together, phenotypically different β cell subpopulations are present at the different ages.

Heterogeneity of Aging Markers in β Cells

To extend our results to the protein level, paraffin sections were stained and analyzed in parallel such that differences in staining intensities reflect differences in protein. There was marked heterogeneity between islets and between the cells within an islet. IGF1R showed enhanced staining in islets of 6.5-month-old and 1.5-year-old mice (Figures 3A and 3B), whereas consistent with it being a marker of younger β cells, KCNQ5 protein was expressed at higher levels at 2 months than at older ages (Figures 3A and 3C). Intensity of insulin staining showed marked variability at each age with a decrease in the 1.5-year-old group (Figure 3D). The membrane location of IGF1R and KCNQ5 was confirmed with costaining with

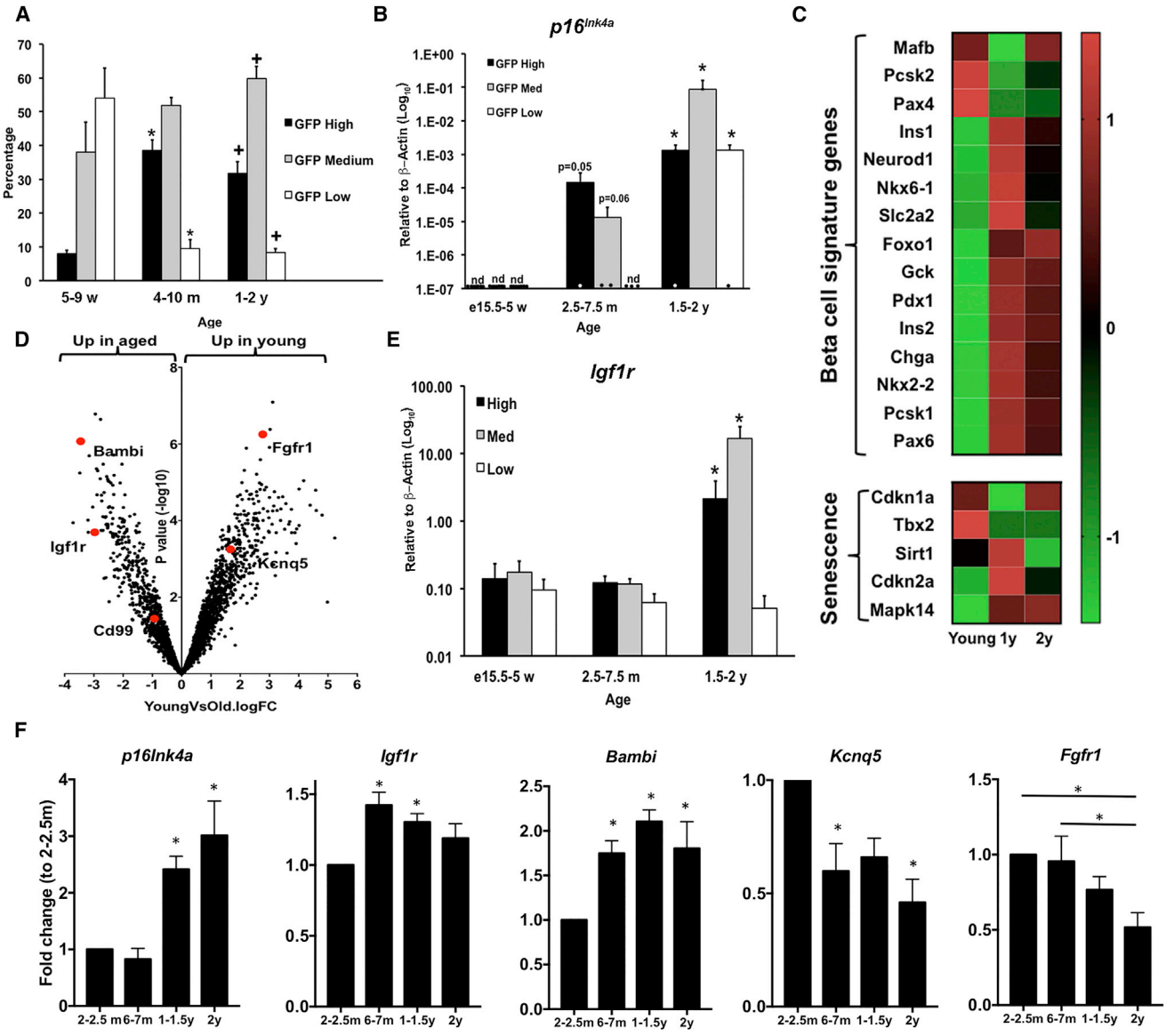

Figure 2. Heterogeneity Patterns of β Cells Change with Age as Seen with FACS Analysis of GFP+ Cells and Measurement of Aging Markers

(A) Based on GFP intensity, there are subpopulations of β cells that change with age. 5–9 weeks, n = 3; 4–10 months, n = 7; 1–2 years, n = 8. *p < 0.04 compared to previous age group; +p < 0.04 to 5–9 weeks. Mean ± SEM.

(B) With age, these subpopulations have increasing expression of *p16*^{Ink4a}, supporting the notion of aging heterogeneity. E15.5–5 weeks, n = 7; 2.5–7.5 months, n = 3; 1.5–2 years, n = 3. For p16^{Ink4a}: ANOVA < 0.0001; *p < 0.0001 to youngest group. ND, not detected. Mean ± SEM.

(C) Heatmaps of expression data from microarrays of β cells of MIP:GFP mice showing changes in key β cell and senescence signature genes (see Figure S3).

(D) Volcano plot of differentially expressed cell surface genes (see Table S1).

(E) Expression of *Igf1r* mRNA increased in GFP$^{high/medium}$ cells at 1.5–2 years. Same samples as for *p16*^{ink4a}. (F) Potential aging surface markers verified by qPCR on isolated islets: *p16*^{Ink4a}, *Igf1r*, *Bambi*, *Kcnq5*, and *Fgfr1*. Samples were from individual mice; n = 10–18 per age; *p < 0.05 with respect to previous age. Mean ± SEM.

E-Cadherin (Figure S5). Using the INKATTAC model, costaining of IGF1R and the reporter of *p16* expression FLAG was seen in a subset of β cells in 4- to 6-month-old mice (Figure S1F). Importantly, age-dependent increases in IGF1R immunostaining intensity were seen in human islets (Figure 3F; Figure S6A). Notably, no staining of IGF1R was found in fetal islets (19- to 22-week gestation).

β Cells Expressing IGF1R Are Senescent and Have Dysfunctional Secretion

To evaluate potential functional differences between β cells expressing IGF1R and those that do not, we used FACS to sort IGF1R^{positive} and^{negative} populations (Figure 3F) The percentage of IGF1R^{positive} increased as the age of the animal increased (Figure 3G). By qPCR, *p16*^{Ink4a} mRNA levels were 50-fold higher in

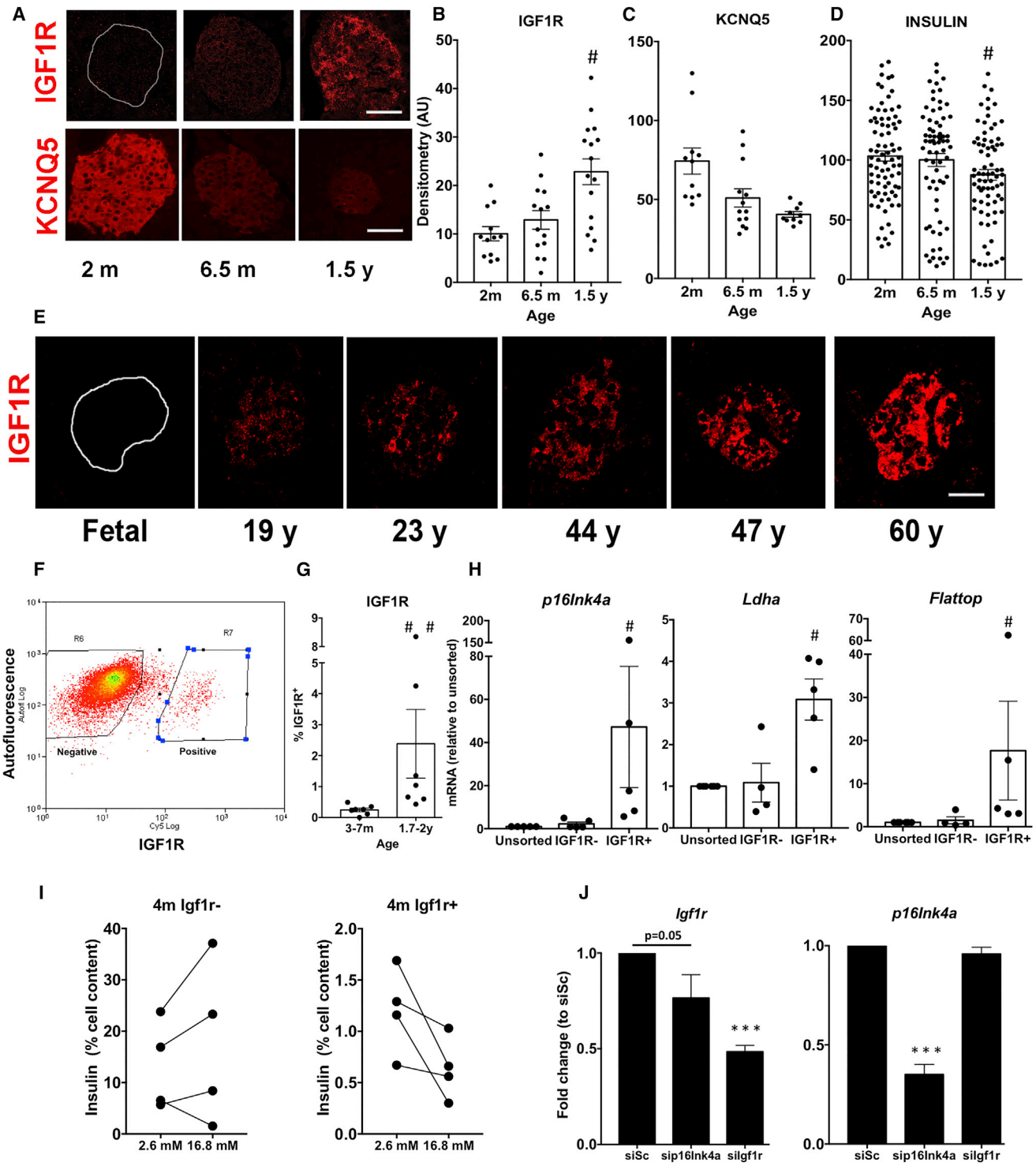

Figure 3. Islet Heterogeneity for Markers of Aging in Mouse and Human Pancreas

(A) By immunostaining, increased IGF1R and decreased KCNQ5 were found in islets from older mice compared to young.

(B–D) Magnification bar, 25 μm. Intensity of individual islet staining quantified for IGF1R (B), KCNQ5 (C), and insulin (D). n = 3 animals per age. *p < 0.05 with respect to previous age.

(E) Age-dependent IGF1R expression in human islets supports the validity of this marker. Pancreas from 2 donors per decade (aged fetal to 68 years); 15–92 islets/cell clusters per donor; total of 400 human islets. Quantification is given in Figure S6A. Magnification bar, 25 μm.

(F) FACS plot showing sorting by IGF1R for β cells.

(G) Percentage of IGF1R+ β cells per age. n = 7 independent cell preparations.

(legend continued on next page)

IGF1R^{positive} cells than in either IGF1R^{negative} or unsorted subpopulations (Figure 3H); both *Ldha* and *Flattop* were also higher in IGF1R^{positive} cells. Functionally, IGF1R^{positive} cells secreted less insulin at 16.8 mM glucose than IGF1R^{negative} cells even when from 4-month-old mice (Figure 3I; Figure S7C), much as seen in older β cells (Figure 1G; Table 1).

Given the expression of *p16^{Ink4a}* in IGF1R^{positive} cells, we knocked down the expression of each in the β cell line MIN6 to test for possible interaction (Figure 3J). When *siP16^{Ink4a}* was used, *Igf1r* mRNA was decreased. However, the knockdown of *Igf1r* had no effect on *p16* mRNA levels. These data suggest that *p16^{Ink4a}* expression may lead to IGF1R expression, supporting the notion that IGF1R truly marks senescent β cells.

Aging Heterogeneity within β Cells

To further examine the simultaneous presence of differentially aged β cells at any given time, we tested two known senescence markers. First, using nuclear localization of p53BP1 protein (Campisi and d'Adda di Fagagna, 2007; Tornovsky-Babeay et al., 2014), we found as mice aged β cells increased p53BP1 protein (Figure 4A), with 50% β cells costaining for IGF1R and p53BP1 at 6.5 months increasing to 100% at 2 years (Figure 4B), a further validation of IGF1R as a β cell aging marker. Then to correlate the GFP subpopulations identified by FACS (Figure 2) with these aging markers, pancreatic sections of MIP-GFP mice at different ages were stained for GFP, P53BP1, and IGF1R (Figure 4C; Figures S7A and S7B). In 6-month-old mice, most, if not all, β (insulin+) cells expressed GFP but showed heterogeneous expression when the antibody concentration was not saturated. With age there was an increased proportion of GFP^{low} insulin + cells. These GFP^{low} β cells tended to have nuclear p53BP1+ β cells and high IGF1R, suggesting that in old animals GFP^{low} β cells included a senescent subpopulation.

Second, we used senescence-associated acidic β-galactosidase activity to identify and isolate senescent β cells. FACS sorting (Figure 4D) showed β-Gal activity to be a continuum; the active subopulation was smaller in 6-month-old compared to 1.5-year-old mice (Figure 4E). Nonetheless, B-Gal^{positive} β cells from both ages had increased expression of both *Igf1r* and *p16Ink4a* mRNA compared to the negative β cells from the same animals (Figure 4F).

Aging Heterogeneity between Islets

Heterogeneity of aging marker among β cells within an islet was greatest in the 6- to 9-month-old mice. What was surprising was the heterogeneity between islets: within the same section, adjacent islets could be positive or negative for IGF1R, CD99, or KCNQ5 (Figures 5A–5D). To better characterize this heterogeneity between individual islets, we characterized single islets handpicked for similar size (150 μm diameter) from 1.5-year-old mice. Even though these single islets had insulin content varying by less than 10% (Figure 5E), their *Igf1r* and *Kcnq5* mRNA levels varied 800% (Figures 5F and 5G). This finding indicates that β cells of differentially aged islets can maintain their insulin stores.

Acceleration of the Appearance of Aging Markers in β Cells by Insulin Resistance

To evaluate whether metabolic stress could induce cellular aging independent of chronological age, 7-month-old C57BL/6J mice were treated for a week with insulin receptor antagonist S961 and as previously described (Yi et al., 2013) showed hyperglycemia and hyperinsulinemia (Figures 6A and 6B). Islets from S961-treated mice had significantly increased *p16^{Ink4a}* and *Bambi* mRNA levels (Figure 6C), and *Igf-1r* mRNA had a tendency to increase. With only 1 week of treatment and 2 weeks recovery, these changes reversed. Then using a model of chronic ER stress, Ins2^{Akita}(Akita) mice (20-week-old heterozygotes), we found *Igf1r* mRNA increased and both *p16^{Ink4a}* and *Bambi* mRNA tended to increase in isolated islets compared to wild-type controls (Figure 6D). Together these results indicate that the appearance of aging markers in β cells can be induced by metabolic stress.

Yet, hyperglycemia or glucose toxicity was not solely responsible for the appearance of the aging marker IGF1R. We examined INK-ATTAC mice in which a fragment of the *p16^{Ink4a}* gene promoter that is transcriptionally active in senescent but not in non-senescent cells drives both GFP reporter and Flag-tagged protein products allowing the identification of senescent cells within a heterogeneous population (Baker et al., 2016; Baker et al., 2008; Baker et al., 2011). These mice remain glucose tolerant even at 1 year (Figures S1A and S1B). In insulin secretion studies, islets from old (1.7–2 years) mice showed increased basal insulin release with equal stimulated release compared to islets from those at 4 months old (Figure S1C). Even so, at 10 months there was heterogeneity of both GFP and FLAG (Figure 6E) expression as well as age-related changes in *Igf1r* and *Kcnq5* mRNA and protein (Figure 6F; Figures S1D and S1E). Moreover, costaining of IGF1R and FLAG in a subset of β cells could be identified in pancreas from 4- to 6-month-old mice. Thus, aging itself is responsible for the changing phenotype but metabolic stress, whether insulin resistance or chronic ER stress, can accelerate the aging process.

Increased IGF1R and P53BP1 in Human β Cells in T2D

To extend our findings to human, we first examined our previously published microarray data on laser capture microdissected β cells from 10 T2D and 10 age-matched non-diabetic controls (Marselli et al., 2010). *IGF1R* mRNA was significantly higher ($p = 0.007$) in β cells from T2D than from controls. Using an in silico approach on recently published papers, *IGF1R* mRNA was significantly correlated with HbA1c in the Fadista (Fadista et al., 2014) PNAS study on islets from 89 human donors. *Bambi* was significantly upregulated in β cells from patients with T2D when compared with non-diabetic donors (Segerstolpe et al., 2016; Xin et al., 2016). In our own work, we

(H) IGF1R+ β cells express higher *p16^{Ink4a}*, *Ldha*, and *Flattop* mRNA as compared to unsorted. n = 5 samples, each pooled from 3–7 1.5- to 2-year-old mice. #$p < 0.05$.

(I) GSIS profiles comparing IGF1R− and IGF1R+ subpopulations from 4 independent cell preparations of 4-month-old mice.

(J) Knockdown experiments in MIN6 cells transfected with *p16^{Ink4a}*, *Igf1r*, or scrambled siRNA (siSc) show p16^{ink4a} affects *Igf1r* expression. n = 3 independent experiments in triplicate. Mean ± SEM.

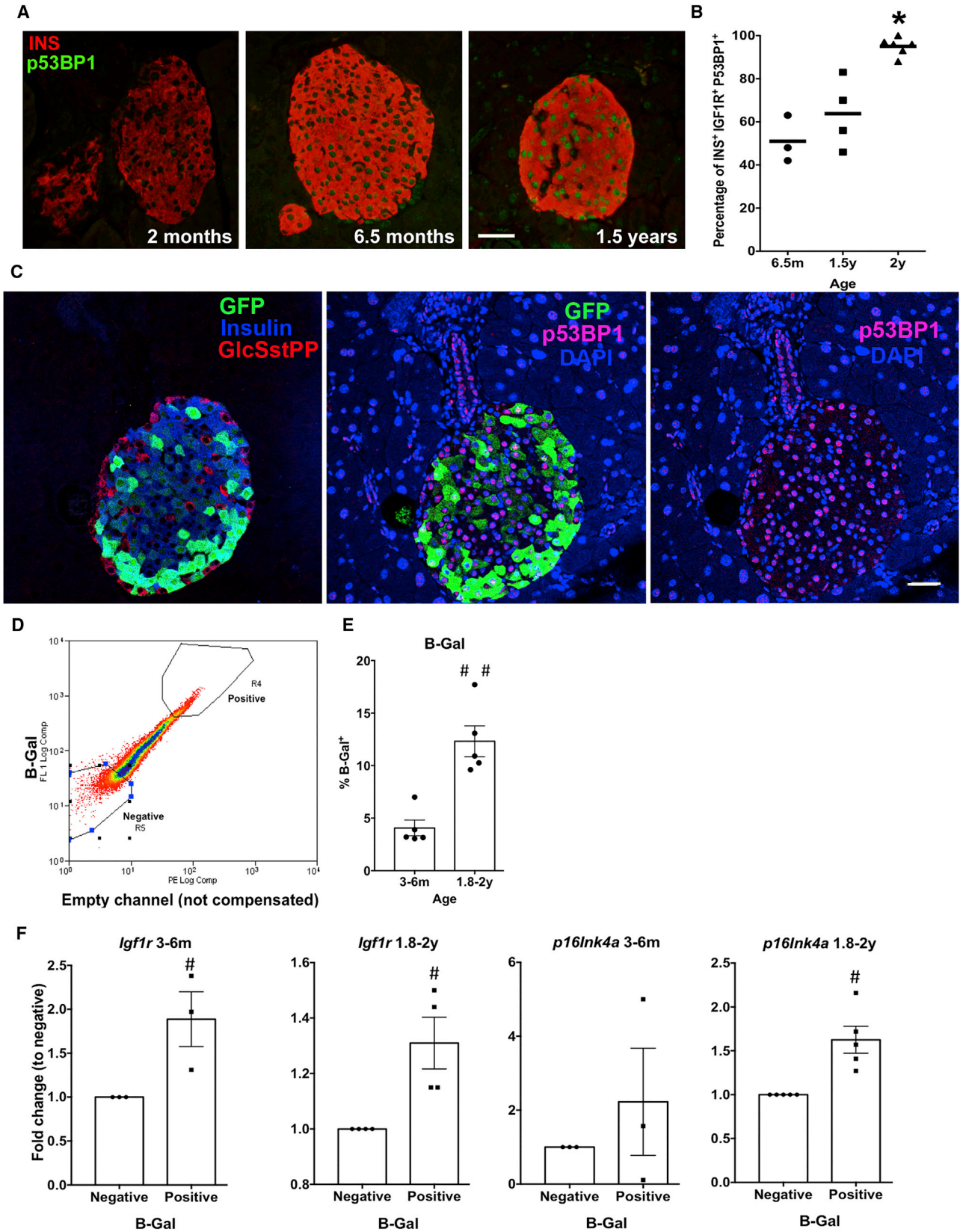

(legend on next page)

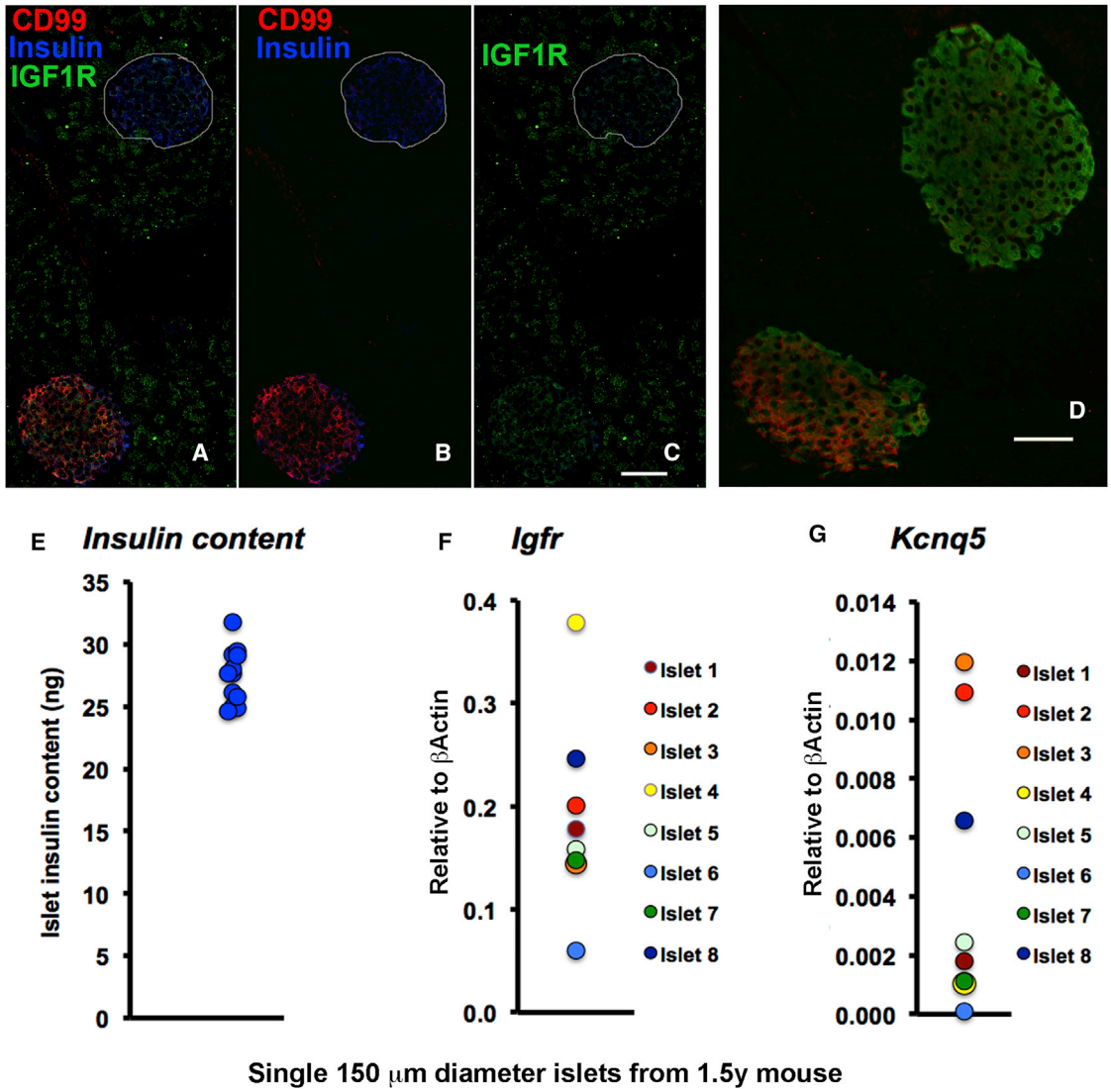

Figure 5. Islet Heterogeneity at Both Protein and mRNA Levels

(A–G) Adjacent islets showed heterogeneous staining of aging markers CD99 and IGF1R (merged channels, A and B; split channels, C) and KCNQ5 (D) indicating islet heterogeneity in adult pancreas. Magnification bar, 50 μm. Heterogeneity of islets was further supported by similar insulin content (E) and marked differences in single islet mRNA content for *Igf1r* (F) and *Kcnq5* (G). Handpicked 150 μM diameter islets: for RNA, 8 islets from same 1.5-year-old mouse; for insulin content, 12 islets, 4 from each of 3 1.5-year-old mice. Individual islet values are shown.

found consistently greater immunostaining intensity of IGF1R in β cells in sections from 3 T2D than from age-matched non-diabetic controls (Figure S6B). In a panel of nPOD samples of T2D and age-matched controls, most donors by age 20 had a considerable number of β cells expressing nuclear p53BP1 without differences in the number of negative cells (Figures 6C and 6D); with age, the percentage of high-intensity nuclei increased (Figure 6E). While it seems that obesity and diabetes are associated

Figure 4. Senescent β Cells Increase in Proportion through Adulthood

(A) Representative images for the senescence marker nuclear P53BP1 in β cells across ages. Magnification bar, 25 μm.

(B) Cellular co-localization of IGF1R and p53BP1 increased with age.

(C) Representative images of adjacent sections of islet from 1-year-old MIP:GFP mouse costained for GFP, insulin, and glucagon/somatostatin/pancreatic polypeptide or for GFP, p53BP1, and DAPI showing p53BP1+ cells are mostly GFP^{low}insulin+. Magnification bar, 30 μm.

(D) FACS plot showing sorting criteria for β cells stained for acidic β-galactosidase (B-Gal) activity.

(E) Proportion of $B\text{-}Gal^{positive}$ β cells increased with age. n = 5 independent preparations, each pooled of 3–5 mice.

(F) $B\text{-}Gal^{positive}$ and $B\text{-}Gal^{negative}$ subpopulations from mature (3–6 months, n = 3) and aged (1.8–2 years, n = 4) mice show higher *Igf1r* and $p16^{Ink4a}$ mRNA levels in B-Gal+ cells at both ages. Data normalized to negative cells. #$p < 0.05$. Mean ± SEM.

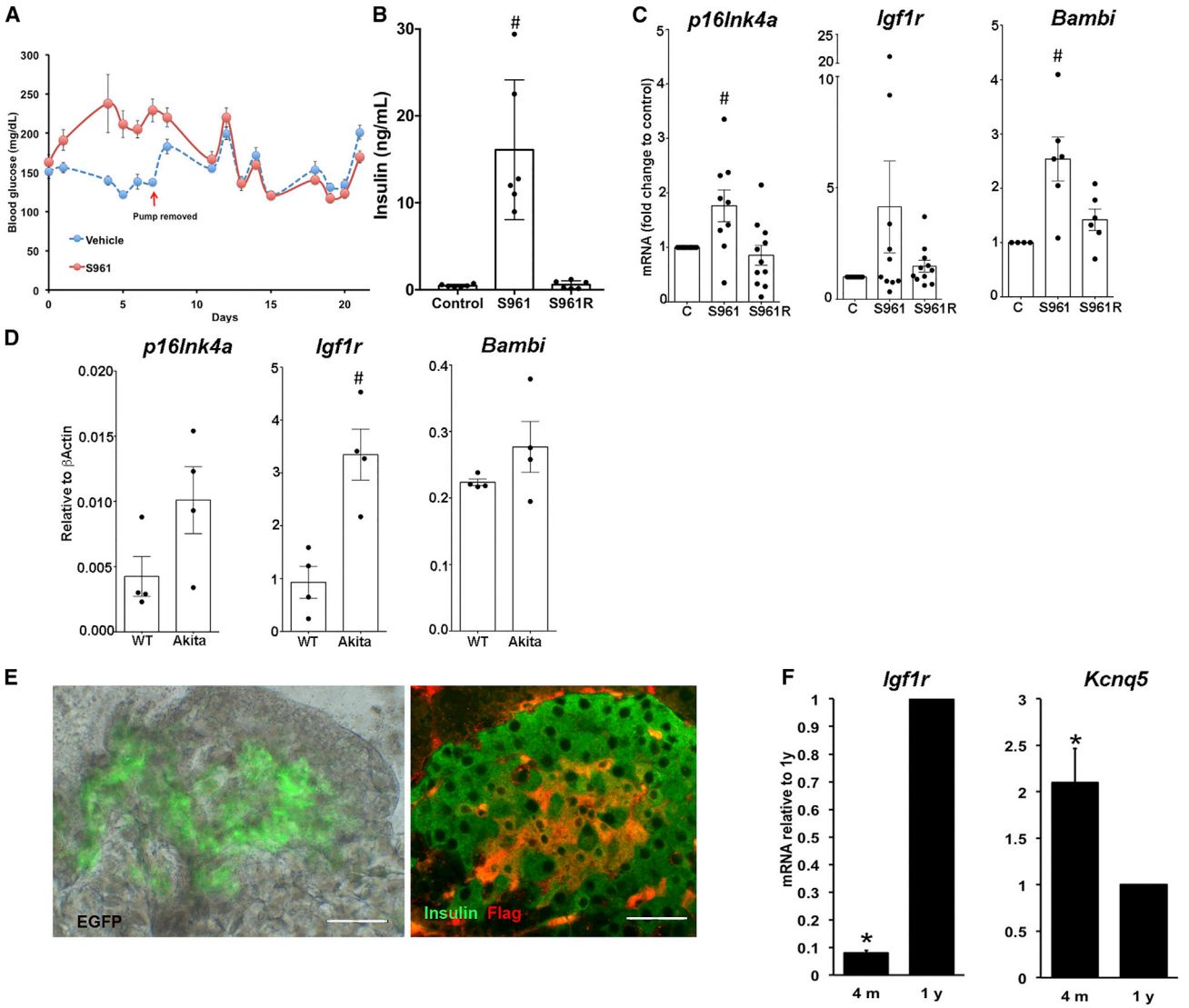

Figure 6. Acceleration of the Appearance of Aging Markers in β Cells by Insulin Resistance and Metabolic Stress

(A and B) In 7-month-old C57BL/6J mice, 7 days of S961 administration induced hyperglycemia (A) and hyperinsulinemia (B), which were reversed by a 2-week recovery period.

(C) Islets of these mice had increased expression of $p16^{Ink4a}$, *Igf1r*, and *Bambi* mRNA that reversed in a 2-week recovery period. Data are related to control values. n = 4–12 mice/group; #p < 0.01.

(D) In islets from $Ins2^{Akita}$ (Akita) mice, a model of ER stress, *Igf1r* mRNA increased and both $p16^{Ink4a}$ and *Bambi* mRNA tended to increase, compared to wild-type (WT). n = 4 mice/group; #p < 0.005.

(E and F) Islets from INK-ATTAC mice show heterogeneity of both GFP and FLAG protein at 10 months (E) as well as age-related changes in *Igf1r* and *Kcnq5* mRNA (F). n = 4 mice/age. *p < 0.02. Magnification bar, 40 μm. Mean ± SEM.

with an increased proportion of high-intensity P53BP1 staining, the great variability among human donors will necessitate a far larger study with groups of similar age and BMI.

DISCUSSION

In the present study we have identified new age markers of β cells. As expected, there was considerable heterogeneity among individual β cells in the expression of these markers, but very surprisingly, there were also remarkable differences among islets. Additionally, we found that the aging process can be accelerated by increased insulin demand. We conclude that the varying age of the individual β cells could be the basis for their heterogeneity.

β cells are known to have slow turnover and a relatively long lifespan (rodents 2–3 months) (Finegood et al., 1995), but this low rate of growth is sufficient to allow sustained β cell mass expansion over the first 7 months in rats (Montanya et al., 2000). There are several mechanisms, such as proliferation, hypertrophy, and neogenesis (Bonner-Weir, 2000) that increase β cell mass to meet the secretory demand as well as adaptations that increase the function of individual β cells (Liu et al., 2000).

Since the β cell population is dynamic, there must be the simultaneous presence of young, adult, senescent, and dying β cells at any adult age (Weir and Bonner-Weir, 2013). These differing populations may have different functional characteristics that impact overall glucose homeostasis. One of the characteristics of functional immaturity is high insulin secretion at low glucose levels as well as diminished ability of the β cell to increase insulin secretion in response to high glucose levels (Blum et al., 2012). Intriguingly, *Flattop*, the newly identified marker of mature β cells, was not expressed in 20% of β cells of adult mice (Bader et al., 2016), the same percentage of rodent adult β cells reported to be non-responsive to glucose (Salomon and Meda, 1986; Van Schravendijk et al., 1992).

As shown in the present study, as C57BL/6J mice age, impaired glucose tolerance develops as well as changes in β cell function. These functional changes are characterized by an increase in basal insulin secretion, impaired glucose-stimulated insulin secretion, along with functional loss of subpopulations of cells that respond to high glucose concentrations. This age-related change in function was accompanied by an increase in $p16^{Ink4a}$, a known marker of β cell aging and by a new marker of β cell aging found in this study, *Igf1r*. By immunostaining, islets that expressed IGF1R had higher expression of p53BP1. When these presumed older cells expressing IGF1R were selected by flow cytometry, their insulin secretory response to high glucose levels was impaired, suggesting that aged β cells are dysfunctional compared to their younger ($IGF1R^{negative}$) counterparts from the same mice. It is also worth mentioning that the $IGF1R^{positive}$ subpopulation was particularly vulnerable to combined stress of dispersion and FACS, such that a 17% of the population appeared to die selectively in response to the procedure. From our microarray analysis, the apoptosis pathway and p53 signaling pathway were ranked 7 and 3, respectively, when comparing β cells isolated from 2-year-old mice with those obtained from young or 1-year-old mice. These results support the idea that older β cells are more fragile and therefore more likely to die in response to a variety of insults or stimuli.

Further support of IGF1R as an aging marker comes from our siRNA experiments that indicate that $p16^{Ink4a}$ expression may lead to IGF1R expression. Using another well-recognized marker of senescent cells, β-galactosidase activity to FACS sort subpopulations, we found that the proportion of $β\text{-}GAL^{positive}$ β cells increased from 6 months to 1.5 years, and at both ages, the positive cells had higher *Igf1r* and *p16* mRNA expression than the negative cells from the same animals.

Our findings are in contrast to a recent study in which induction of $p16^{Ink4a}$ for 10 days in β cells of 3- to 4-week-old transgenic mice resulted in both markers of senescence and increased function of β cells (Helman et al., 2016), leading to their conclusion of a novel functional benefit of senescence in β cells. However, the β cells of 5- to 6-week-old mice are not yet fully mature; islets from 3-week-old rats are glucose responsive but without the robustness of a 2- to 3-month-old rat (Bliss and Sharp, 1992). Another study on epigenome changes in β cells from adolescent (4–6 weeks) and old (16–20 months) also found age-related changes in function and increased *Igf1r* mRNA in old β cells but without significant changes in *Cdkn2a* ($p16^{ink4a}$) (Avrahami et al., 2015). They concluded that the left shift in glucose sensitivity in old mice (46.2% of old β cells versus 13.3% of young responding to 5 mM glucose) indicated improved function of old β cells. However, it may be that the perceived increased sensitivity of the "old" cells was due to their being compared to a population of immature cells.

With these newly identified markers coupled with known markers of cell senescence, $p16^{Ink4a}$, p53BP1, and acidic β-galactosidase, we have shown the presence of subpopulations of differentially aged β cells at any given time in adult mice. These markers accumulated as the age of the mice increased, and this was similarly found for β cells in human pancreases. This is not unexpected given that the replicative capacity of β cells decreases with age in both rodents (Scaglia et al., 1997) and humans (Gregg et al., 2012; Kushner, 2013), which likely results in the overall population being older and having more senescent cells. Even so, the high frequency of nuclear p53BP1 in islets of humans even as young as 20 was surprising. Moreover, this change in proliferative capacity of murine β cells fits nicely with our microarray results in which we saw the greatest changes in gene expression between β cells isolated from young and 1-year-old mice. The changes between β cells from 1- and 2-year-old mice were less pronounced and may reflect the increasing accumulation of senescent cells.

The heterogeneity seen in expression of the markers within individual islets as well as among islets within the same pancreas was striking. The finding of β cell heterogeneity was not unexpected since various aspects of heterogeneity have been previously demonstrated (Pipeleers et al., 1994); in the present study, secretory heterogeneity was again seen, and it was clear that both newly identified and known aging markers are present only in some cells.

We conclude that the varying cellular age of the β cells may be one factor for the basis for their heterogeneity. Heterogeneity of β cells may be influenced by other factors; some of the functional and gene expression changes are reminiscent of immature or dedifferentiated β cells. β cell dedifferentiation has many meanings in the field. We have previously reported (Jonas et al., 1999; Weir et al., 2013) that hyperglycemia can lead to a change in β cell phenotype and function, often called glucotoxicity. Here we see many changes occurring with age in both the glucose-intolerant C57BL/6J and the normoglycemic INKATTAC mice, such that these changes are unlikely to be dependent on glycemic levels. One could consider both the immature and the senescent β cell as dedifferentiated as compared to the archetypical mature β cells, but our interpretation is that β cells at different life stages do not have identical phenotypes. Recently, a subpopulation of β cells (1%–10%) called "hub" cells were identified in young adult mice; they were highly metabolic but with many characteristics of immature β cells (Johnston et al., 2016). While in the young MIP:GFP mice, GFP^{low} β cells may be immature, in older mice most of the GFP^{low} β cells are likely, rather, to be senescent as seen by their preponderance of being nuclear p53BP1+ β cells. This is clearly supported by our microarray analysis of β cells obtained from young mice that are still undergoing maturation, and a subsequent aging population that accumulates. Even though some changes might seem similar between the immature and the senescent cells that could point to dedifferentiation (*Mafb*, *Ins1*, *NeuroD*, *Nkx6.1*, and *Glut2*), the overall gene expression profile is very different between

these two groups as shown by other β cell hallmark genes (*Pdx1*, *Ins2*, *Pcsk1*) as well as by the cellular senescence gene set. These data support the presence of different phenotypes at different life stages of a β cell.

The heterogeneity of islets was very surprising. We have long known that there are a variety of histological differences among islets in normal and T2D pancreases; however, here we found marked differences in islets with both immunostaining of pancreatic sections and gene expression measurements of individual islets. It is tempting to attribute these differences to variations in the age of these islets; however, there could be other possibilities, including the concept that gene and protein expression in all β cells of a particular islet might change in a coordinated way over time. Perhaps there are islets in humans that are temporarily functionally active or inactive, as has been described in rats in a provocative study (Olsson and Carlsson, 2011) suggesting that under normal conditions, up to 25% of pancreatic islets were functionally dormant, but that these "sleeping" islets could be activated in response to demand for more insulin secretion.

Our new markers of aging were selected without regard to their possible function to identify the differently aged subpopulations of β cells within a pancreas. Yet, the markers of age identified in this study may be involved in the mechanisms related to the age-associated functional decline of β cells. IGF1R is of particular interest since the insulin/IGF-1 signaling pathway has a major influence on lifespan across species (Barbieri et al., 2003). Having multiple markers is important to provide a "senescent β cell signature" since senescence is seen not as a static endpoint but as, a multi-step evolving process (van Deursen, 2014).

Our findings that aging and the development of diabetes are associated with the appearance of markers for aging in β cells fit with generally held concepts. In an acute insulin resistance model induced by the insulin receptor antagonist S961, the development of both hyperglycemia and hyperinsulinemia after 7 days of treatment coincided with increased islet expression of the aging markers. Similar increases in the aging markers were seen in both 5-month-old diabetic Akita mice and aging or diabetic human pancreases. Importantly, these data show that the increased metabolic stress of insulin resistance resulted in accelerated aging of β cells, thus providing insights as to how increases in β cell apoptosis might be occurring before glucose levels start to rise during progression to diabetes. This fits well with the finding that the state of impaired fasting glucose is associated with a 40% reduction in β cell mass (Butler et al., 2003). A related important question is whether old β cells have less insulin secretory capacity than younger β cells; our findings provide support for this concept.

In summary, the present study has identified new markers of aging in β cells, whose pattern of expression suggests that the varying life cycle stage of the β cells is the basis for their heterogeneity. Additionally, we found that the expression of these and other markers can be accelerated by metabolic stress. This finding provides insight into how insulin resistance might accelerate the decline of β cells. In addition, striking heterogeneity among islets was found, which opens up new ways to think about islet biology and the pathogenesis of T2D.

STAR★METHODS

Detailed methods are provided in the online version of this paper and include the following:

- KEY RESOURCES TABLE
- CONTACT FOR REAGENT AND RESOURCE SHARING
- EXPERIMENTAL MODEL AND SUBJECT DETAILS
  - Mice
  - Human tissue
  - Cell lines
- METHOD DETAILS
  - Assessment of glucose homeostasis in animals
  - FACS
  - Microarray
  - Insulin secretion in vitro
  - Quantitative real-time PCR (QPCR)
  - Immunostaining and morphometric evaluation
  - S961 treatment
  - Knockdown Experiments
- QUANTIFICATION AND STATISTICAL ANALYSIS
- DATA AND SOFTWARE AVAILABILITY

SUPPLEMENTAL INFORMATION

Supplemental Information includes seven figures and one table and can be found with this article online at http://dx.doi.org/10.1016/j.cmet.2017.03.015.

AUTHOR CONTRIBUTIONS

C.A.-M. and S.B.-W. conceived the project and wrote the manuscript; C.A.-M., M.v.H., M.M., T.B.L., C.C., J.H.-L., B.A.S., and J.W.J. researched data; J.M.D. and A.E. performed the bioinformatics; J.V.D. provided INK:ATTAC mice and advice; G.C.W. provided critical discussions and edited the manuscript. All authors reviewed the manuscript.

ACKNOWLEDGMENTS

We thank Dr. C.R. Kahn for helpful and insightful discussion of this project; we thank both Drs. J. Winnay and Kahn for RNA from islets from the $Ins2^{Akita}$ mice. This study was supported by grants from the NIH (R01 DK093909 [S.B.-W.], P30 DK036836 Joslin Diabetes Research Center [DRC], and P30 DK057521 BADRC P&F PI [C.A.-M.]), the Diabetes Research and Wellness Foundation, and an important group of private donors. Some human tissue sections were provided by the Network for Pancreatic Organ Donors with Diabetes (nPOD), a collaborative research project sponsored by JDRF. Organ Procurement Organizations (OPO) partnering with nPOD to provide research resources are listed at http://www.jdrfnpod.org/for-partners/npod-partners/.

Received: August 12, 2016
Revised: January 10, 2017
Accepted: March 21, 2017
Published: April 4, 2017

REFERENCES

Aguayo-Mazzucato, C., Sanchez-Soto, C., Godinez-Puig, V., Gutiérrez-Ospina, G., and Hiriart, M. (2006). Restructuring of pancreatic islets and insulin secretion in a postnatal critical window. PLoS ONE *1*, e35.

Aguayo-Mazzucato, C., Koh, A., El Khattabi, I., Li, W.C., Toschi, E., Jermendy, A., Juhl, K., Mao, K., Weir, G.C., Sharma, A., and Bonner-Weir, S. (2011). Mafa expression enhances glucose-responsive insulin secretion in neonatal rat beta cells. Diabetologia *54*, 583–593.

Avrahami, D., Li, C., Zhang, J., Schug, J., Avrahami, R., Rao, S., Stadler, M.B., Burger, L., Schübeler, D., Glaser, B., and Kaestner, K.H. (2015). Aging-Dependent Demethylation of Regulatory Elements Correlates with Chromatin State and Improved β Cell Function. Cell Metab. *22*, 619–632.

Bader, E., Migliorini, A., Gegg, M., Moruzzi, N., Gerdes, J., Roscioni, S.S., Bakhti, M., Brandl, E., Irmler, M., Beckers, J., et al. (2016). Identification of proliferative and mature β-cells in the islets of Langerhans. Nature *535*, 430–434.

Baker, D.J., Perez-Terzic, C., Jin, F., Pitel, K.S., Niederländer, N.J., Jeganathan, K., Yamada, S., Reyes, S., Rowe, L., Hiddinga, H.J., et al. (2008). Opposing roles for p16Ink4a and p19Arf in senescence and ageing caused by BubR1 insufficiency. Nat. Cell Biol. *10*, 825–836.

Baker, D.J., Wijshake, T., Tchkonia, T., LeBrasseur, N.K., Childs, B.G., van de Sluis, B., Kirkland, J.L., and van Deursen, J.M. (2011). Clearance of p16Ink4a-positive senescent cells delays ageing-associated disorders. Nature *479*, 232–236.

Baker, D.J., Childs, B.G., Durik, M., Wijers, M.E., Sieben, C.J., Zhong, J., Saltness, R.A., Jeganathan, K.B., Verzosa, G.C., Pezeshki, A., et al. (2016). Naturally occurring p16(Ink4a)-positive cells shorten healthy lifespan. Nature *530*, 184–189.

Barbieri, M., Bonafè, M., Franceschi, C., and Paolisso, G. (2003). Insulin/IGF-I-signaling pathway: an evolutionarily conserved mechanism of longevity from yeast to humans. Am. J. Physiol. Endocrinol. Metab. *285*, E1064–E1071.

Bliss, C.R., and Sharp, G.W. (1992). Glucose-induced insulin release in islets of young rats: time-dependent potentiation and effects of 2-bromostearate. Am. J. Physiol. *263*, E890–E896.

Blum, B., Hrvatin, S.S., Schuetz, C., Bonal, C., Rezania, A., and Melton, D.A. (2012). Functional beta-cell maturation is marked by an increased glucose threshold and by expression of urocortin 3. Nat. Biotechnol. *30*, 261–264.

Bonner-Weir, S. (2000). Perspective: Postnatal pancreatic beta cell growth. Endocrinology *141*, 1926–1929.

Bosco, D., and Meda, P. (1991). Actively synthesizing beta-cells secrete preferentially after glucose stimulation. Endocrinology *129*, 3157–3166.

Butler, A.E., Janson, J., Bonner-Weir, S., Ritzel, R., Rizza, R.A., and Butler, P.C. (2003). Beta-cell deficit and increased beta-cell apoptosis in humans with type 2 diabetes. Diabetes *52*, 102–110.

Campisi, J., and d'Adda di Fagagna, F. (2007). Cellular senescence: when bad things happen to good cells. Nat. Rev. Mol. Cell Biol. *8*, 729–740.

Chen, H., Gu, X., Su, I.H., Bottino, R., Contreras, J.L., Tarakhovsky, A., and Kim, S.K. (2009). Polycomb protein Ezh2 regulates pancreatic beta-cell Ink4a/Arf expression and regeneration in diabetes mellitus. Genes Dev. *23*, 975–985.

Dhawan, S., Tschen, S.I., and Bhushan, A. (2009). Bmi-1 regulates the Ink4a/Arf locus to control pancreatic beta-cell proliferation. Genes Dev. *23*, 906–911.

Dorrell, C., Schug, J., Canaday, P.S., Russ, H.A., Tarlow, B.D., Grompe, M.T., Horton, T., Hebrok, M., Streeter, P.R., Kaestner, K.H., and Grompe, M. (2016). Human islets contain 4 distinct subtypes of beta cells. Nat. Commun. *7*, 11756.

Fadista, J., Vikman, P., Laakso, E.O., Mollet, I.G., Esguerra, J.L., Taneera, J., Storm, P., Osmark, P., Ladenvall, C., Prasad, R.B., et al. (2014). Global genomic and transcriptomic analysis of human pancreatic islets reveals novel genes influencing glucose metabolism. Proc. Natl. Acad. Sci. USA *111*, 13924–13929.

Finegood, D.T., Scaglia, L., and Bonner-Weir, S. (1995). Dynamics of beta-cell mass in the growing rat pancreas. Estimation with a simple mathematical model. Diabetes *44*, 249–256.

Freeman, H.C., Hugill, A., Dear, N.T., Ashcroft, F.M., and Cox, R.D. (2006). Deletion of nicotinamide nucleotide transhydrogenase: a new quantitive trait locus accounting for glucose intolerance in C57BL/6J mice. Diabetes *55*, 2153–2156.

Gepts, W., and Lecompte, P.M. (1981). The pancreatic islets in diabetes. Am. J. Med. *70*, 105–115.

Gotoh, M., Maki, T., Satomi, S., Porter, J., Bonner-Weir, S., O'Hara, C.J., and Monaco, A.P. (1987). Reproducible high yield of rat islets by stationary in vitro digestion following pancreatic ductal or portal venous collagenase injection. Transplantation *43*, 725–730.

Gregg, B.E., Moore, P.C., Demozay, D., Hall, B.A., Li, M., Husain, A., Wright, A.J., Atkinson, M.A., and Rhodes, C.J. (2012). Formation of a human β-cell population within pancreatic islets is set early in life. J. Clin. Endocrinol. Metab. *97*, 3197–3206.

Guo, N., Parry, E.M., Li, L.S., Kembou, F., Lauder, N., Hussain, M.A., Berggren, P.O., and Armanios, M. (2011). Short telomeres compromise β-cell signaling and survival. PLoS ONE *6*, e17858.

Hara, M., Wang, X., Kawamura, T., Bindokas, V.P., Dizon, R.F., Alcoser, S.Y., Magnuson, M.A., and Bell, G.I. (2003). Transgenic mice with green fluorescent protein-labeled pancreatic beta -cells. Am. J. Physiol. Endocrinol. Metab. *284*, E177–E183.

Helman, A., Klochendler, A., Azazmeh, N., Gabai, Y., Horwitz, E., Anzi, S., Swisa, A., Condiotti, R., Granit, R.Z., Nevo, Y., et al. (2016). p16(Ink4a)-induced senescence of pancreatic beta cells enhances insulin secretion. Nat. Med. *22*, 412–420.

Hiriart, M., and Ramirez-Medeles, M.C. (1991). Functional subpopulations of individual pancreatic B-cells in culture. Endocrinology *128*, 3193–3198.

Hiriart, M., Sanchez-Soto, M.C., Ramirez-Medeles, M.C., and Malaisse, W.J. (1995). Functional heterogeneity of single pancreatic beta-cells stimulated by L-leucine and the methyl ester of succinic or glutamic acid. Biochem. Mol. Med. *54*, 133–137.

Johnston, N.R., Mitchell, R.K., Haythorne, E., Pessoa, M.P., Semplici, F., Ferrer, J., Piemonti, L., Marchetti, P., Bugliani, M., Bosco, D., et al. (2016). Beta Cell Hubs Dictate Pancreatic Islet Responses to Glucose. Cell Metab. *24*, 389–401.

Jonas, J.C., Sharma, A., Hasenkamp, W., Ilkova, H., Patanè, G., Laybutt, R., Bonner-Weir, S., and Weir, G.C. (1999). Chronic hyperglycemia triggers loss of pancreatic beta cell differentiation in an animal model of diabetes. J. Biol. Chem. *274*, 14112–14121.

Karaca, M., Castel, J., Tourrel-Cuzin, C., Brun, M., Géant, A., Dubois, M., Catesson, S., Rodriguez, M., Luquet, S., Cattan, P., et al. (2009). Exploring functional beta-cell heterogeneity in vivo using PSA-NCAM as a specific marker. PLoS ONE *4*, e5555.

Katsuta, H., Aguayo-Mazzucato, C., Katsuta, R., Akashi, T., Hollister-Lock, J., Sharma, A.J., Bonner-Weir, S., and Weir, G.C. (2012). Subpopulations of GFP-marked mouse pancreatic β-cells differ in size, granularity, and insulin secretion. Endocrinology *153*, 5180–5187.

Kaufman, R.J. (2011). Beta-cell failure, stress, and type 2 diabetes. N. Engl. J. Med. *365*, 1931–1933.

Kiekens, R., In 't Veld, P., Mahler, T., Schuit, F., Van De Winkel, M., and Pipeleers, D. (1992). Differences in glucose recognition by individual rat pancreatic B cells are associated with intercellular differences in glucose-induced biosynthetic activity. J. Clin. Invest. *89*, 117–125.

King, A.J., Fernandes, J.R., Hollister-Lock, J., Nienaber, C.E., Bonner-Weir, S., and Weir, G.C. (2007). Normal relationship of beta- and non-beta-cells not needed for successful islet transplantation. Diabetes *56*, 2312–2318.

Köhler, C.U., Olewinski, M., Tannapfel, A., Schmidt, W.E., Fritsch, H., and Meier, J.J. (2011). Cell cycle control of β-cell replication in the prenatal and postnatal human pancreas. Am. J. Physiol. Endocrinol. Metab. *300*, E221–E230.

Koopman, R.J., Mainous, A.G., 3rd, Diaz, V.A., and Geesey, M.E. (2005). Changes in age at diagnosis of type 2 diabetes mellitus in the United States, 1988 to 2000. Ann. Fam. Med. *3*, 60–63.

Krishnamurthy, J., Torrice, C., Ramsey, M.R., Kovalev, G.I., Al-Regaiey, K., Su, L., and Sharpless, N.E. (2004). Ink4a/Arf expression is a biomarker of aging. J. Clin. Invest. *114*, 1299–1307.

Krishnamurthy, J., Ramsey, M.R., Ligon, K.L., Torrice, C., Koh, A., Bonner-Weir, S., and Sharpless, N.E. (2006). p16INK4a induces an age-dependent decline in islet regenerative potential. Nature *443*, 453–457.

Kushner, J.A. (2013). The role of aging upon β cell turnover. J. Clin. Invest. *123*, 990–995.

Ling, Z., Wang, Q., Stangé, G., In't Veld, P., and Pipeleers, D. (2006). Glibenclamide treatment recruits beta-cell subpopulation into elevated and sustained basal insulin synthetic activity. Diabetes *55*, 78–85.

Liu, Y.Q., Nevin, P.W., and Leahy, J.L. (2000). beta-cell adaptation in 60% pancreatectomy rats that preserves normoinsulinemia and normoglycemia. Am. J. Physiol. Endocrinol. Metab. *279*, E68–E73.

Marselli, L., Thorne, J., Dahiya, S., Sgroi, D.C., Sharma, A., Bonner-Weir, S., Marchetti, P., and Weir, G.C. (2010). Gene expression profiles of Beta-cell enriched tissue obtained by laser capture microdissection from subjects with type 2 diabetes. PLoS ONE *5*, e11499.

Montanya, E., Nacher, V., Biarnés, M., and Soler, J. (2000). Linear correlation between beta-cell mass and body weight throughout the lifespan in Lewis rats: role of beta-cell hyperplasia and hypertrophy. Diabetes *49*, 1341–1346.

Olsson, R., and Carlsson, P.O. (2011). A low-oxygenated subpopulation of pancreatic islets constitutes a functional reserve of endocrine cells. Diabetes *60*, 2068–2075.

Peng, S.W., Zhu, L.Y., Chen, M., Zhang, M., Li, D.Z., Fu, Y.C., Chen, S.R., and Wei, C.J. (2009). Heterogeneity in mitotic activity and telomere length implies an important role of young islets in the maintenance of islet mass in the adult pancreas. Endocrinology *150*, 3058–3066.

Pipeleers, D.G. (1992). Heterogeneity in pancreatic beta-cell population. Diabetes *41*, 777–781.

Pipeleers, D., Kiekens, R., Ling, Z., Wilikens, A., and Schuit, F. (1994). Physiologic relevance of heterogeneity in the pancreatic beta-cell population. Diabetologia *37* (*Suppl 2*), S57–S64.

Ritchie, M.E., Phipson, B., Wu, D., Hu, Y., Law, C.W., Shi, W., and Smyth, G.K. (2015). limma powers differential expression analyses for RNA-sequencing and microarray studies. Nucleic Acids Res. *43*, e47.

Salomon, D., and Meda, P. (1986). Heterogeneity and contact-dependent regulation of hormone secretion by individual B cells. Exp. Cell Res. *162*, 507–520.

Scaglia, L., Cahill, C.J., Finegood, D.T., and Bonner-Weir, S. (1997). Apoptosis participates in the remodeling of the endocrine pancreas in the neonatal rat. Endocrinology *138*, 1736–1741.

Schäffer, L., Brand, C.L., Hansen, B.F., Ribel, U., Shaw, A.C., Slaaby, R., and Sturis, J. (2008). A novel high-affinity peptide antagonist to the insulin receptor. Biochem. Biophys. Res. Commun. *376*, 380–383.

Schuit, F.C., In't Veld, P.A., and Pipeleers, D.G. (1988). Glucose stimulates proinsulin biosynthesis by a dose-dependent recruitment of pancreatic beta cells. Proc. Natl. Acad. Sci. USA *85*, 3865–3869.

Schuppin, G.T., Bonner-Weir, S., Montana, E., Kaiser, N., and Weir, G.C. (1993). Replication of adult pancreatic-beta cells cultured on bovine corneal endothelial cell extracellular matrix. In Vitro Cell. Dev. Biol. Anim. *29A*, 339–344.

Segerstolpe, Å., Palasantza, A., Eliasson, P., Andersson, E.M., Andréasson, A.C., Sun, X., Picelli, S., Sabirsh, A., Clausen, M., Bjursell, M.K., et al. (2016). Single-Cell Transcriptome Profiling of Human Pancreatic Islets in Health and Type 2 Diabetes. Cell Metab. *24*, 593–607.

Tian, L., Greenberg, S.A., Kong, S.W., Altschuler, J., Kohane, I.S., and Park, P.J. (2005). Discovering statistically significant pathways in expression profiling studies. Proc. Natl. Acad. Sci. USA *102*, 13544–13549.

Tornovsky-Babeay, S., Dadon, D., Ziv, O., Tzipilevich, E., Kadosh, T., Schyr-Ben Haroush, R., Hija, A., Stolovich-Rain, M., Furth-Lavi, J., Granot, Z., et al. (2014). Type 2 diabetes and congenital hyperinsulinism cause DNA double-strand breaks and p53 activity in β cells. Cell Metab. *19*, 109–121.

Tschen, S.I., Dhawan, S., Gurlo, T., and Bhushan, A. (2009). Age-dependent decline in beta-cell proliferation restricts the capacity of beta-cell regeneration in mice. Diabetes *58*, 1312–1320.

van Deursen, J.M. (2014). The role of senescent cells in ageing. Nature *509*, 439–446.

Van Schravendijk, C.F., Kiekens, R., and Pipeleers, D.G. (1992). Pancreatic beta cell heterogeneity in glucose-induced insulin secretion. J. Biol. Chem. *267*, 21344–21348.

Weir, G.C., and Bonner-Weir, S. (2013). Islet β cell mass in diabetes and how it relates to function, birth, and death. Ann. N Y Acad. Sci. *1281*, 92–105.

Weir, G.C., Aguayo-Mazzucato, C., and Bonner-Weir, S. (2013). β-cell dedifferentiation in diabetes is important, but what is it? Islets *5*, 233–237.

Westermark, G.T., and Westermark, P. (2013). Islet amyloid polypeptide and diabetes. Curr. Protein Pept. Sci. *14*, 330–337.

Xin, Y., Kim, J., Okamoto, H., Ni, M., Wei, Y., Adler, C., Murphy, A.J., Yancopoulos, G.D., Lin, C., and Gromada, J. (2016). RNA sequencing of single human islet cells reveals type 2 diabetes genes. Cell Metab. *24*, 608–615.

Yi, P., Park, J.S., and Melton, D.A. (2013). Betatrophin: a hormone that controls pancreatic β cell proliferation. Cell *153*, 747–758.

STAR★METHODS

KEY RESOURCES TABLE

REAGENT or RESOURCE	SOURCE	IDENTIFIER
Antibodies		
IGF1r 1:100 IF; 1:10 FACS	Santa Cruz	rabbit; sc-713
IGF1r 1:100	Abcam	chicken; ab32823
CD99 1:1000	Bioss	rabbit; bs-2523R
Kcnq5 1:500	Alomone Labs	rabbit;APC-155
p53BP1 1:400	Bethyl	rabbit; A300-272A
GFP 1:3000	Aves Lab	chicken;GFP-1020
FLAG 1:500	Sigma Aldrich	mouse; F1804
Insulin 1:500	Dako	guinea pig; A0564
IgG (rabbit) 1:200	Jackson Immunoresearch	donkey; Alexa 488, −594, Cy5
IgG (chicken) 1:200	Abcam	goat; dylight-488
IgG (Guinea pig) 1:200	Jackson Immunoresearch	donkey; Alexa 488, −594
IgG (rabbit) 1:200 IF: 1:100 FACS	Jackson Immunoresearch	donkey; Biotin-SP
Streptavidin 1:200	Jackson Immunoresearch	AMCA
Propidium iodide 1:10^7	eBioscience	00-6990
Biological Samples		
Non diabetic; 22 years; M; 21.9 BMI; formaldehyde-fixed, paraffin-embedded sections of human pancreas (organ donor)	NPOD	6001
Non diabetic; 22 years; F; 20.7 BMI; formaldehyde-fixed, paraffin-embedded sections of human pancreas (organ donor)	NPOD	6179
Non diabetic; 38 years; M; 30.5 BMI; formaldehyde-fixed, paraffin-embedded sections of human pancreas (organ donor)	NPOD	6254
Non diabetic; 42 years; M; 31 BMI; formaldehyde-fixed, paraffin-embedded sections of human pancreas (organ donor)	NPOD	6019
Non diabetic; 59 years; F; 24.8 BMI; formaldehyde-fixed, paraffin-embedded sections of human pancreas (organ donor)	NPOD	6017
Non diabetic; 68 years; F; 23.7 BMI; formaldehyde-fixed, paraffin-embedded sections of human pancreas (organ donor)	NPOD	6012
T2D; 13 years; F; 34.1 BMI; formaldehyde-fixed, paraffin-embedded sections of human pancreas (organ donor)	NPOD	6308
T2D; 18.8 years; F; 39.1 BMI; formaldehyde-fixed, paraffin-embedded sections of human pancreas (organ donor)	NPOD	6059
T2D; 21 years; F; 40 BMI; formaldehyde-fixed, paraffin-embedded sections of human pancreas (organ donor)	NPOD	6110
T2D; 20 years; M;37.8 BMI; formaldehyde-fixed, paraffin-embedded sections of human pancreas (organ donor)	NPOD	6252
T2D; 33 years; M; 30.2 BMI; formaldehyde-fixed, paraffin-embedded sections of human pancreas (organ donor)	NPOD	6028
T2D; 45 years; F; 30.4 BMI; formaldehyde-fixed, paraffin-embedded sections of human pancreas (organ donor)	NPOD	6127
T2D; 49 years; F; 36.1 BMI; formaldehyde-fixed, paraffin-embedded sections of human pancreas (organ donor)	NPOD	6189
T2D; 59 years; M; 34.1 BMI; formaldehyde-fixed, paraffin-embedded sections of human pancreas (organ donor)	NPOD	6206

(*Continued on next page*)

Continued

REAGENT or RESOURCE	SOURCE	IDENTIFIER
T2D; 61 years; F; 33.7 BMI; formaldehyde-fixed, paraffin-embedded sections of human pancreas (organ donor)	NPOD	6221
Non diabetic; 65 years; F; 45.6 BMI; formaldehyde-fixed, paraffin-embedded sections of human pancreas (organ donor)	Joslin Clinical Islet Isolation Core	H06-02
Non diabetic; 44 years; F; 26.7 BMI; formaldehyde-fixed, paraffin-embedded sections of human pancreas (organ donor)	Joslin Clinical Islet Isolation Core	H02-03
Non diabetic; 55 years; F; 25.2 BMI; formaldehyde-fixed, paraffin-embedded sections of human pancreas (organ donor)	Joslin Clinical Islet Isolation Core	H01-03
Non diabetic; 54 years; F; 36 BMI; formaldehyde-fixed, paraffin-embedded sections of human pancreas (organ donor)	Joslin Clinical Islet Isolation Core	H06-10
Non diabetic; 43 years; F; 35.8 BMI; formaldehyde-fixed, paraffin-embedded sections of human pancreas (organ donor)	Joslin Clinical Islet Isolation Core	H05-14
Non diabetic; 45 years; F; 21.5 BMI; formaldehyde-fixed, paraffin-embedded sections of human pancreas (organ donor)	Joslin Clinical Islet Isolation Core	H03-17
Non diabetic; 45 years; F; 37.4 BMI; formaldehyde-fixed, paraffin-embedded sections of human pancreas (organ donor)	Joslin Clinical Islet Isolation Core	H06-23
Non diabetic; 46 years; F; 34.8 BMI; formaldehyde-fixed, paraffin-embedded sections of human pancreas (organ donor)	Joslin Clinical Islet Isolation Core	H02-23
Non diabetic; 62 years; F; 22.4 BMI; formaldehyde-fixed, paraffin-embedded sections of human pancreas (organ donor)	Joslin Clinical Islet Isolation Core	H05-03
Non diabetic; 65 years; F; 34 BMI; formaldehyde-fixed, paraffin-embedded sections of human pancreas (organ donor)	Joslin Clinical Islet Isolation Core	H03-16
Non diabetic; 67 years; F; 38.3 BMI; formaldehyde-fixed, paraffin-embedded sections of human pancreas (organ donor)	Joslin Clinical Islet Isolation Core	H03-13
Non diabetic; 68 years; F; 23.8 BMI; formaldehyde-fixed, paraffin-embedded sections of human pancreas (organ donor)	Joslin Clinical Islet Isolation Core	H03-14
Non diabetic; 17 years; M; 23.7 BMI; formaldehyde-fixed, paraffin-embedded sections of human pancreas (organ donor)	Joslin Clinical Islet Isolation Core	H01-12
Non diabetic; 19 years; M; 27 BMI; formaldehyde-fixed, paraffin-embedded sections of human pancreas (organ donor)	Joslin Clinical Islet Isolation Core	H01-04
Non diabetic; 23 years; M; 23.7 BMI; formaldehyde-fixed, paraffin-embedded sections of human pancreas (organ donor)	Joslin Clinical Islet Isolation Core	H01-18
Non diabetic; 28 years; F; 24.9 BMI; formaldehyde-fixed, paraffin-embedded sections of human pancreas (organ donor)	Joslin Clinical Islet Isolation Core	H04-09
Non diabetic; 33 years; M; 24.6 BMI; formaldehyde-fixed, paraffin-embedded sections of human pancreas (organ donor)	Joslin Clinical Islet Isolation Core	H01-14
Non diabetic; 44 years; M; 23.2 BMI; formaldehyde-fixed, paraffin-embedded sections of human pancreas (organ donor)	Joslin Clinical Islet Isolation Core	H03-04

(*Continued on next page*)

Continued

REAGENT or RESOURCE	SOURCE	IDENTIFIER
Non diabetic; 47 years; F; 23.2 BMI; formaldehyde-fixed, paraffin-embedded sections of human pancreas (organ donor)	Joslin Clinical Islet Isolation Core	H01-06
Non diabetic; 53 years; M; 25.9 BMI; formaldehyde-fixed, paraffin-embedded sections of human pancreas (organ donor)	Joslin Clinical Islet Isolation Core	H01-16
Non diabetic; 56 years; F; 21.1 BMI; formaldehyde-fixed, paraffin-embedded sections of human pancreas (organ donor)	Joslin Clinical Islet Isolation Core	H01-17
Non diabetic; 60 years; M; 24.7 BMI; formaldehyde-fixed, paraffin-embedded sections of human pancreas (organ donor)	Joslin Clinical Islet Isolation Core	H02-19
fetal 18- to 20-week gestation	Advanced Bioscience Resources, Inc	Y92A
fetal 18-week gestation	Advanced Bioscience Resources, Inc	Y93B
Chemicals, Peptides, and Recombinant Proteins		
S961 was a generous gift from Dr. Lauge Schaffer	Novo Nordisk, Denmark	N/A
Critical Commercial Assays		
Cellular Senescence Live Cell Analysis Assay Kit (SA-β-gal, Fluorometric)	Enzo Life Sciences	enz-kit 130-0010
SMARTpool: ON-TARGETplus Cdkn2a siRNA	Dharmacon	L-043107-00-0005
SMARTpool: ON-TARGETplus Igf1r siRNA	Dharmacon	L-056843-00-0005
ON-TARGETplus Non-targeting Pool	Dharmacon	D-001810-10-05
Deposited Data		
Raw microarray data	This paper	GSE72753
Experimental Models: Cell Lines		
MIN6 beta cell line	Dr. Jun-ichi Miyazaki, Osaka University Medical School	N/A
Experimental Models: Organisms/Strains		
C57BL/6J	Jackson	000664
MIP-GFP, bred onto C57BL/6J as in Katsuta et al., 2012	Dr. Manami Hara, Univ Chicago	N/A
INK-ATTAC line 3 congenic, C57Bl6J background	Dr. Jan van Deursen, Mayo Clinic	N/A
Oligonucleotides		
Beta-actin, mouse	Eurofins	5′ACCGTGAAAAGATGACCCAG-3′ 5′GTACGACCAGAGGCATACAG-3′
IGF1r, mouse	Eurofins	5′ATTCTGATGTCTGGTCCTTCG-3′ 5′AGCATATCAGGGCAGTTGTC-3′
CD99, mouse	Eurofins	5′CGTGGTTTTGGCCCTGG-3′ 5′GGTTGGCTTCATGTTGGG-3′
Kcnq5, mouse	Eurofins	5′TGTTTTCTACCATCCCTGAGC-3′ 5′CCTTGCCATCCTCTATAACGAC-3′
Insulin-1, mouse	Genosys	5′CCTGTTGGTGCACTTCCTA-3′ 5′TCTGAAGGTCCCCGGGGCT-3′
$p16^{Ink4a}$, mouse	Eurofins	5′CCCAACGCCCCGAACT-3′ 5′GCAGAAGAGCTGCTACGTGAA-3′
Ldha, mouse	Eurofins	5′GGATGAGCTTGCCCTTGTTGA-3′ 5′GACCAGCTTGGAGTTCGCAGTTA-3′
Fltp, mouse	Eurofins	5′CTGAAGATCCCACCTGCTAAG-3′ 5′CCCATTACAGGCGTTGAGTAG-3′
Software and Algorithms		
Prism 7 software	GraphPad software	https://www.graphpad.com/scientific-software/prism/

CONTACT FOR REAGENT AND RESOURCE SHARING

Further information and requests for resources and reagents should be directed to and will be fulfilled by the Lead Contact, Dr. Susan Bonner-Weir (susan.bonner-weir@joslin.harvard.edu). Requests to use INK-ATTAC mice should be directed to Dr. Jan van Deursen (vanDeursen.Jan@mayo.edu).

EXPERIMENTAL MODEL AND SUBJECT DETAILS

Mice

All experiments were conducted at Joslin Diabetes Center with approval of its Animal Care and Use Committee; mice were kept on a 12-h light/12-h dark cycle with water and food ad libitum. Both male and female mice were used except when noted, and the age of the mice is specified for each experiment. All mice (wild-type, MIP:GFP and INK-ATTAC) were from our colonies: mouse insulin promoter:GFP (MIP-GFP) mice (Hara et al., 2003) were bred onto C57BL/6J background (Katsuta et al., 2012); breeding pairs of INK-ATTAC mice(C57BL/6) were the gift of Dr. Jan van Deursen (Baker et al., 2011). C57BL/6J were from Jackson Labs.

Human tissue

Pancreases from adult brain-dead donors were obtained by the Harvard/Joslin Islet Resource Center; a small piece for quality control assessment was fixed in 4% PFA overnight and embedded in paraffin; additional sections from these blocks were used for this study. Cases were selected to represent different age decades from available tissues. Additional sections of type 2 diabetes and age-matched control donors were obtained from nPOD. Anonymously donated 18-20 wk old fetal pancreas (Advanced Biosciences Resources, Inc) were fixed for 2 hr in 4% PFA for paraffin embedding. All tissues were consented for research and had IRB exempt status (Joslin Diabetes Center IRB). Details of donors are given in Key Resources Table.

Cell lines

For transfection experiments murine beta cell line MIN6 cells were used and maintained in high-glucose Dulbecco's modified Eagle's medium (DMEM-H) supplemented with 15% FBS and 0.05% β-Mercaptoethanol (99% Cell culture tested). These were originally received from Dr. Jun-ichi Miyazaki, Osaka University Medical School.

METHOD DETAILS

Assessment of glucose homeostasis in animals

Body weight and morning fed glucose levels were monitored longitudinally. Blood glucose values were measured using One-Touch glucometer (LifeScan, Milpitas, CA) on blood from tail snip. For intraperitoneal glucose tolerance tests, blood samples from mice fasted overnight (15 h) were collected at 0, 15, 30, 60, 90, and 120 min after an intraperitoneal injection of glucose (2 g/kg body weight). For insulin tolerance tests, mice were fasted for 4 hr, insulin (Humulin R; Eli Lilly, Indianapolis, IN; 0.75 units/kg body weight) injected intraperitoneally, and blood glucose measured at 0, 15, 30, and 60 min.

Pancreas was excised under anesthesia and either fixed in 4% (para)-formaldehyde (PFA) 2h and embedded in paraffin for histology or islets were isolated by collagenase digestion (Gotoh et al., 1987) for 17-18 min, followed by a Ficoll gradient and handpicked for RNA or secretion. Between steps, islets were washed with M199 + 10% NCS. Insulin was measured with a mouse insulin ELISA kit (ALPCO, Salem, NH).

FACS

Isolated islets were dispersed in a solution of 1 mg/ml trypsin (Sigma, St. Louis, MO) and 30 μg/ml DNase (Roche, Mannheim, Germany) and were resuspended in FACS buffer (2% fetal bovine serum (FBS) (Cellgro, Manassas, VA) in PBS). Using a DakoCytomation MoFlo Cytometer (Dako, Ft. Collins, CO), cells were gated according to forward scatter and then sorted as β cells on the basis of higher endogenous fluorescence as shown in Figure S2G (King et al., 2007). Propidium iodide was used to exclude dead cells. For sorting based on surface markers, previous to cell sorting, cells were incubated for 1 hr at 4°C first in blocking solution (normal goat serum in FACS buffer), then with primary antibody (Key Resources Table), followed by 30 min at 4°C in secondary antibody. Sorted cells were collected in FACS buffer and resuspended in culture media (RPMI 10% FBS, 1% Pen/Strep) for attachment and secretion studies or in 100 μL RNA extraction buffer and stored at −80°C. For sorting based on acidic β-galactosidase activity, a fluorescent substrate was used (Enzo Life Sciences enz-kit 130-0010): dispersed islet cells were pretreated with 2 mL of 1x cell pretreatment solution and incubated at 37°C for 2 hr. 10 uL of 200x SA-beta-Gal substrate solution were added to cells in the pretreatment solution and incubated for 1h at 37°C. Cells were then washed with PBS, resuspended in sorting buffer (PBS + 2%FBS) and FACS sorted.

Microarray

β cells from dispersed islets of differently-aged C57BL/6J MIP-GFP mice were purified by FACS (Katsuta et al., 2012) for gene expression profiles using GeneChip Mouse Genome 430 2.0 Array microarrays (Affymetrix, Santa Clara, CA) with n = 3 for Young

(3-9 wk); 4 for 1 y, and 3 for 2 y. The arrays were normalized using robust multi-array average (RMA) and analyzed using a custom script employing the *limma* (Ritchie et al., 2015) and *sigPathway* (Tian et al., 2005) packages in the R software (www.r-project.org).

Insulin secretion in vitro

Insulin secretion was measured by sequential static 1 hr incubations in 2.6 and 16.8 mM glucose in Krebs-Ringer bicarbonate buffer (KRB, 16 mM HEPES and 0.1% BSA, pH 7.4)(Schuppin et al., 1993). This was preceded by a 1h incubation of the islets at 2.6mM at 37°C. Between each incubation, islets were washed with KREBS 2.6mM. Supernatants and cells were frozen until assayed. IGF1R^{positive} and ^{negative} subpopulations were FACS sorted, and incubated overnight for attachment and recovery before static GSIS. Alternatively, we measured insulin secretion of single β cells using the reverse hemolytic plaque assay (RHPA) in which secreted insulin is revealed by the presence of hemolytic plaques around secreting cells. After overnight culture, isolated islet cells were completely dispersed and mixed with protein A-coated sheep erythrocytes (18% suspension) and introduced into a poly-L-lysine-coated glass Cunningham chamber. They were stimulated with 2.6 or 16.8 mmol/l glucose in KRB for 2 hr in the presence of guinea pig anti-insulin antiserum (1:40, generated in our laboratory). This was followed by 30 min incubation with guinea pig complement (1:40; Calbiochem, San Diego, CA, USA) and fixation with glutaraldehyde 2.5%. Secreted insulin was revealed as hemolytic plaques around secreting cells. The percentage of insulin-secreting cells forming plaques and the area of the plaques were measured and multiplied to calculate the secretion index, a measure of the overall secretory activity of β cells under a given condition.

Quantitative real-time PCR (QPCR)

Total RNA isolated with PicoRNA extraction kit (Arcturus) or RNEasy Plus Mini Kit (QIAGEN) was reverse transcribed (SuperScript reverse transcriptase, Invitrogen). QPCR used SYBR green detection and specific primers (Key Resources Table). Samples were normalized to β-actin, and the comparative CT (threshold cycle) method used to calculate gene expression levels.

Immunostaining and morphometric evaluation

Paraffin sections were incubated overnight with primary antibody (Key Resources Table). For each antibody, sections were stained and imaged in parallel such that the staining intensity reflects the protein expression. For quantification, images were captured systematically covering the whole section in confocal mode on a Zeiss LSM 710 microscope. Every cluster of insulin-stained cells (3-7 cells) or islet (8 or more cells)/section was evaluated; sections were coded and read blindly. For each age, 3-4 animals were evaluated for each staining. For human samples, sections from one block from the body of the pancreas from donors as listed in Key Resources Table.

S961 treatment

S961 was a generous gift from Dr. Lauge Schaffer (Novo Nordisk) (Schäffer et al., 2008). Vehicle (PBS or NaCl 0.9%) or 10 nmol S961 was loaded into Alzet osmotic pump 2001 and implanted subcutaneously on the back of mice (Yi et al., 2013) for 7 days. At the end of this period the pump was extracted, and the islets were isolated for analysis immediately or the mice were followed for two weeks before their islets were isolated.

Knockdown Experiments

siRNA against mouse *p16Ink4a*, *Igf1r* and RNA interference-negative control were purchased from Thermo Scientific/Dharmacon (Lafayette, CO). MIN6 cells were plated at 200,000 cells/ well in a 24 well plate. After overnight attachment, they were transfected using DharmaFECT (2.5uL per reaction) and siRNA concentration of 100 nM. After 48 hr transfection, the cells were harvested for RNA and qPCR analysis. Results are presented as fold change to MIN6 cells treated with nonspecific siRNA (siSc).

QUANTIFICATION AND STATISTICAL ANALYSIS

Data are shown as mean ± SEM. Statistical parameters (numbers, p value, etc.) are included in each figure legend. For statistical analysis, unpaired Student's t tests were used to compare two groups, and one-way ANOVA followed by post hoc test for more than two groups. A p value < 0.05 was considered significant. Prism software was used for graphs and statistical analysis (significance and distribution).

DATA AND SOFTWARE AVAILABILITY

The accession number for the genomic data reported in this paper is Gene Expression Omnibus: GSE72753.

Cell Metabolism, Volume *25*

Supplemental Information

β Cell Aging Markers Have Heterogeneous Distribution and Are Induced by Insulin Resistance

Cristina Aguayo-Mazzucato, Mark van Haaren, Magdalena Mruk, Terence B. Lee, Jr., Caitlin Crawford, Jennifer Hollister-Lock, Brooke A. Sullivan, James W. Johnson, Aref Ebrahimi, Jonathan M. Dreyfuss, Jan Van Deursen, Gordon C. Weir, and Susan Bonner-Weir

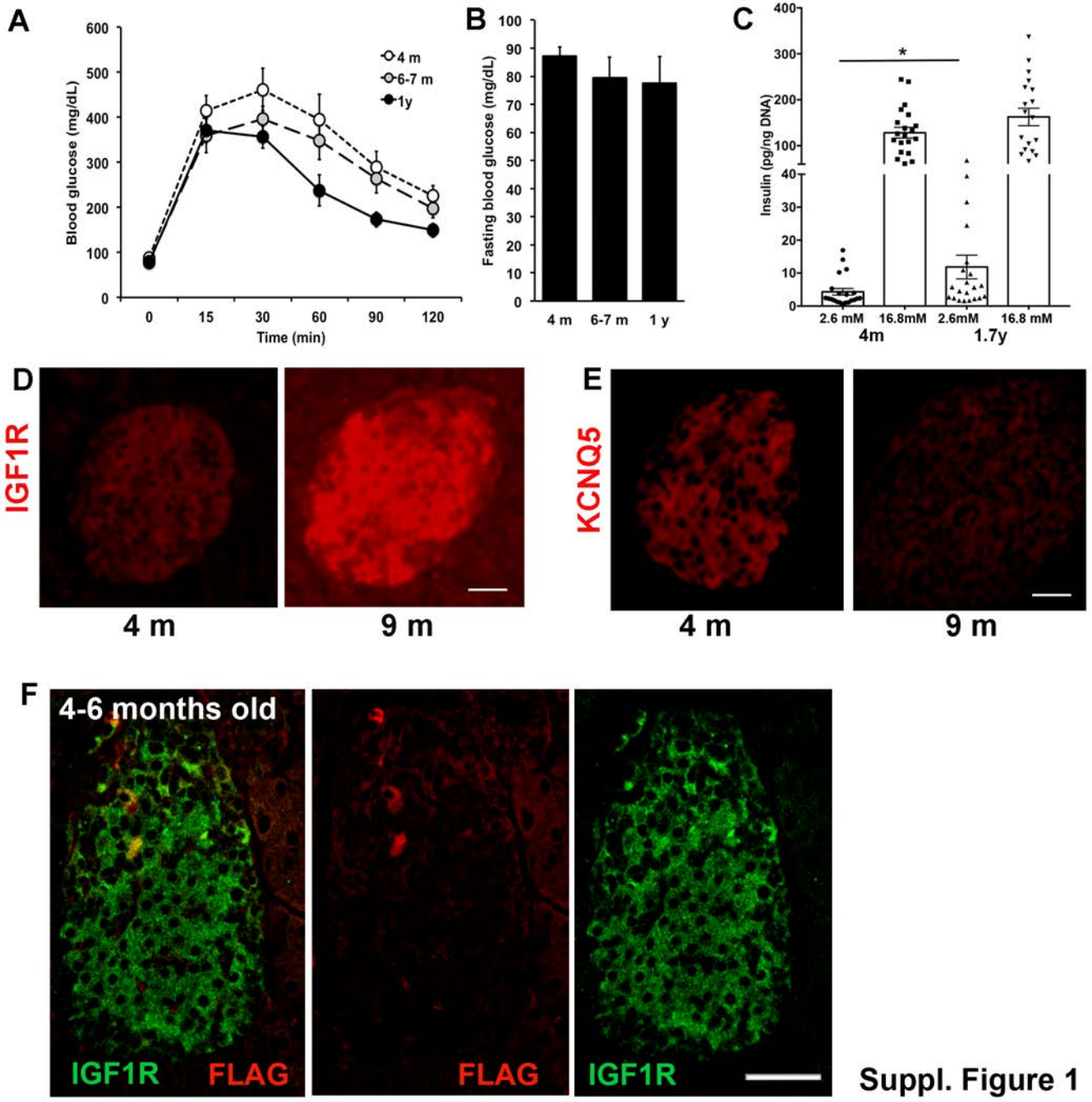

Suppl. Figure 1

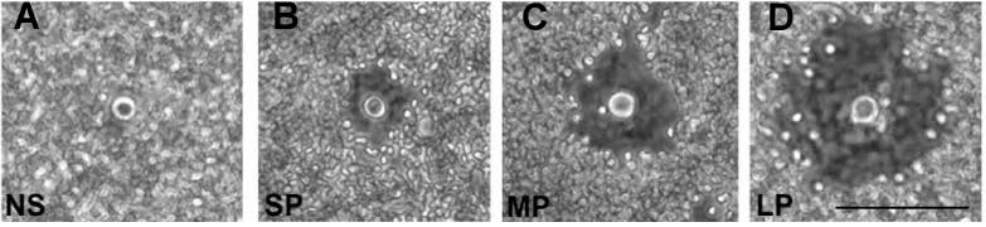

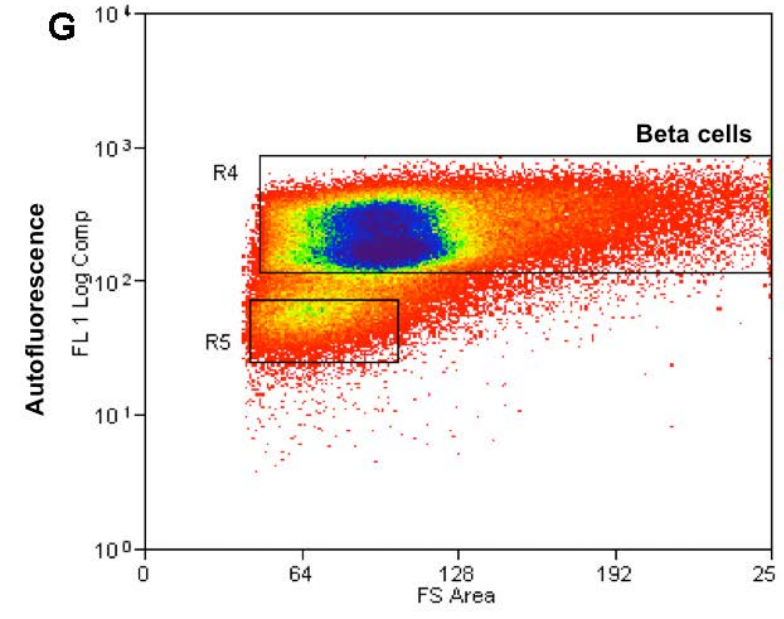

Suppl. Figure 2

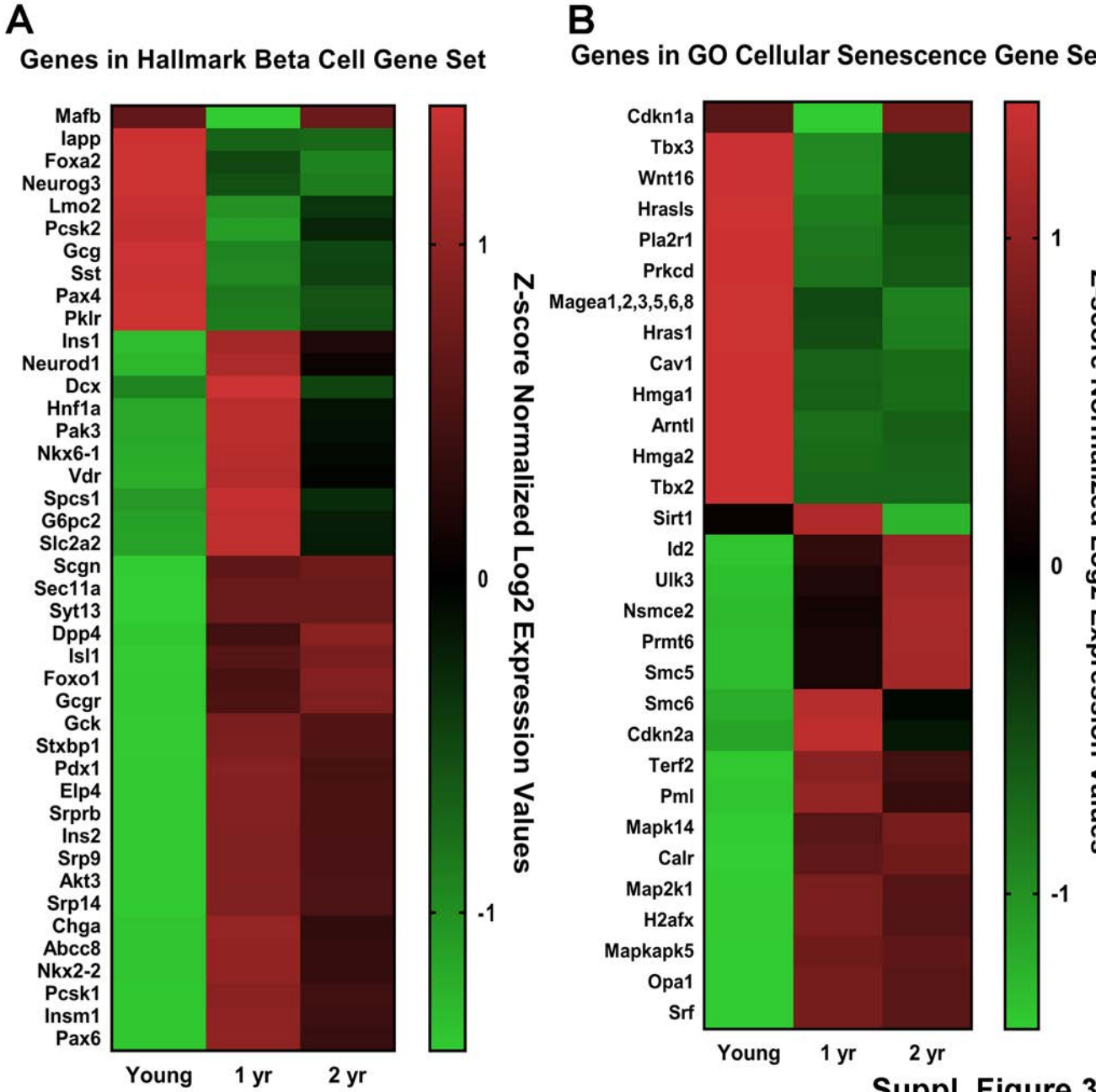

Suppl. Figure 3

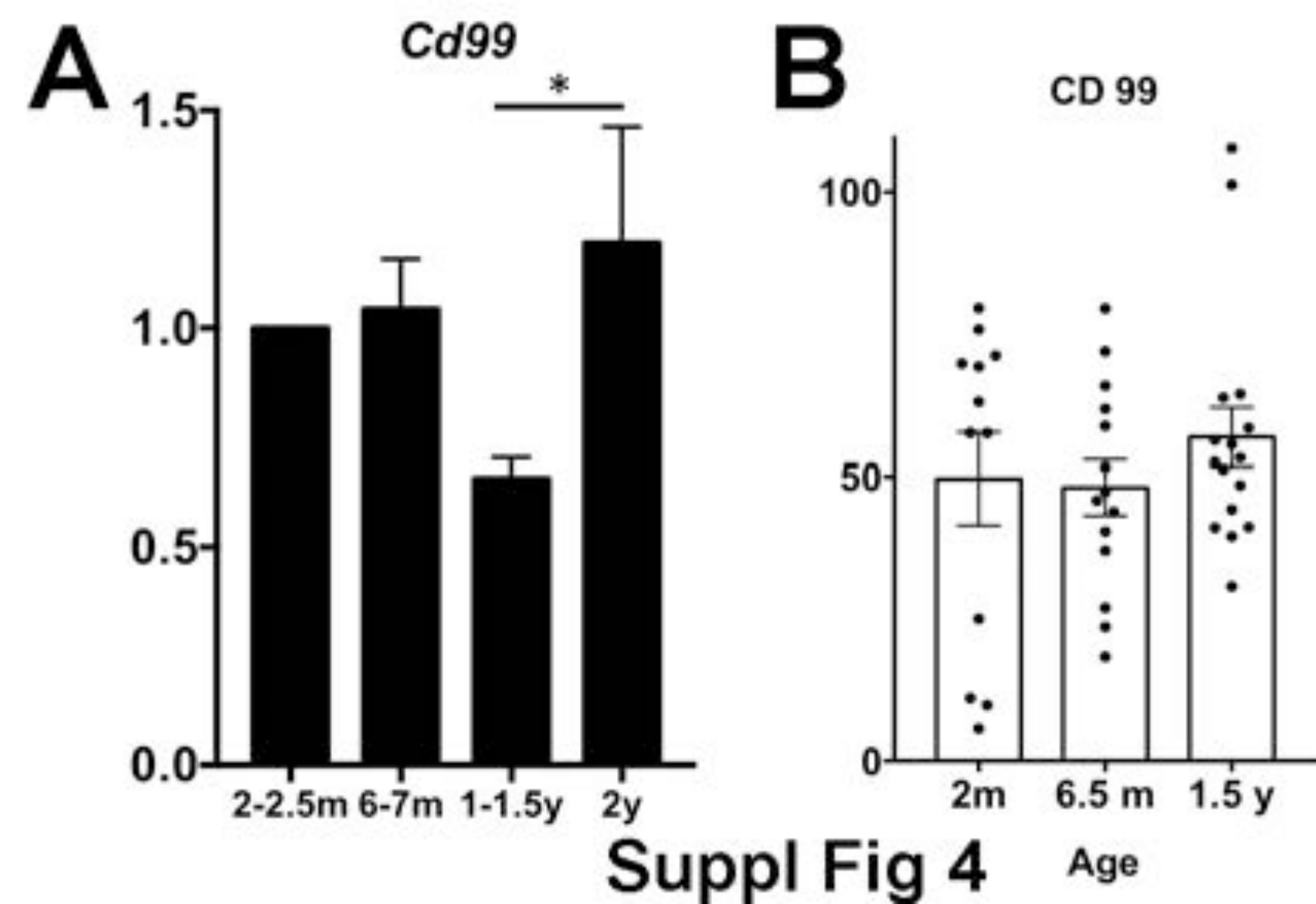

Suppl Fig 4

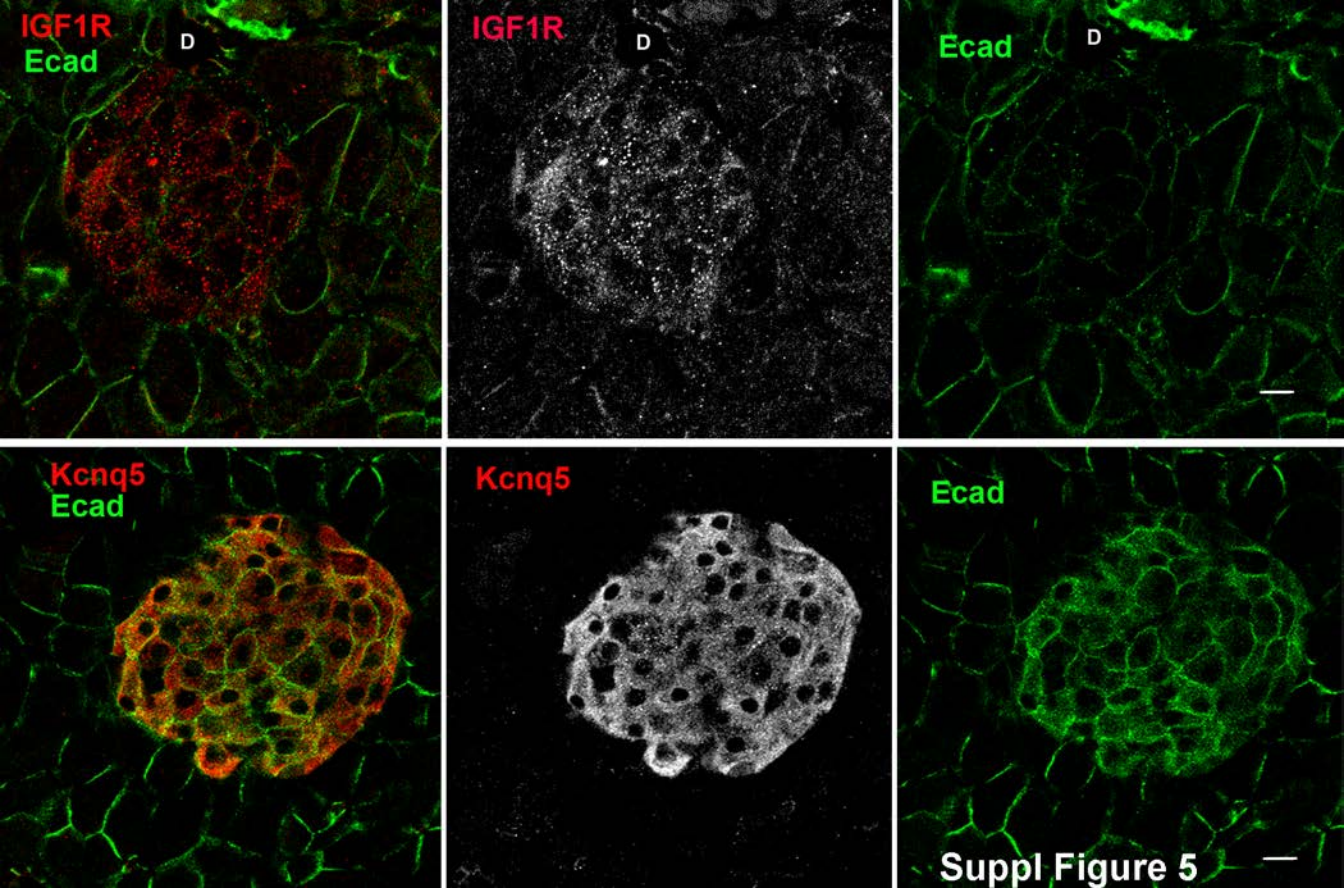
IGF1R
Ecad
D
IGF1R
D
Ecad
D
Kcnq5
Ecad
Kcnq5
Ecad
Suppl Figure 5

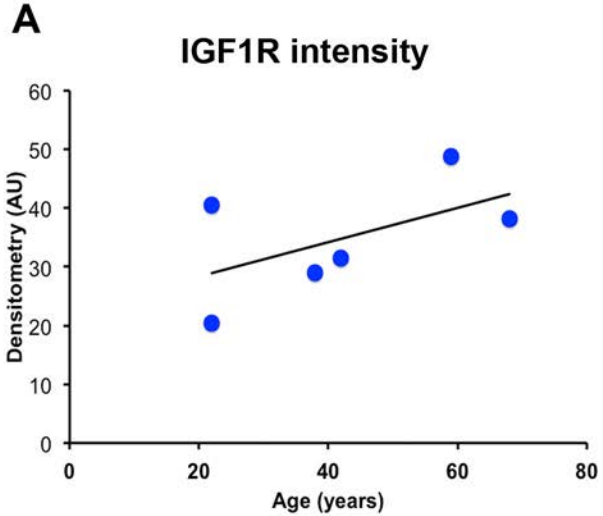

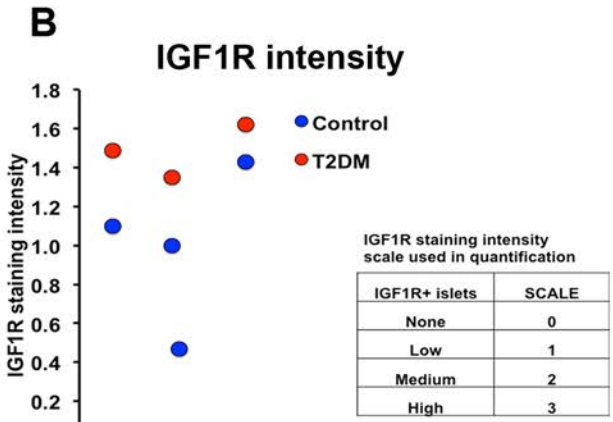

IGF1R staining intensity scale used in quantification

IGF1R+ islets	SCALE
None	0
Low	1
Medium	2
High	3

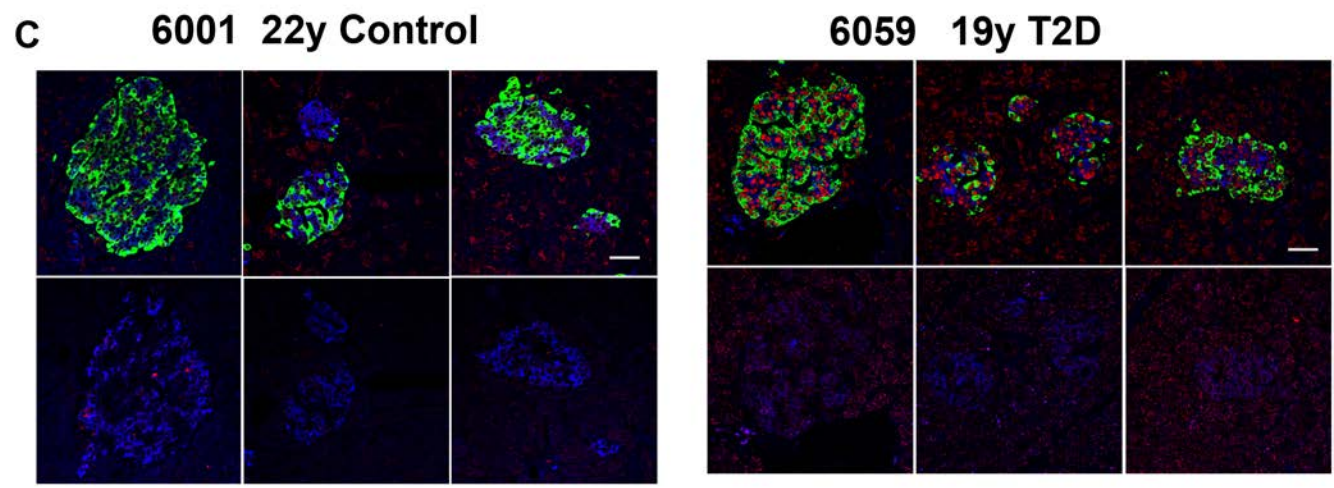

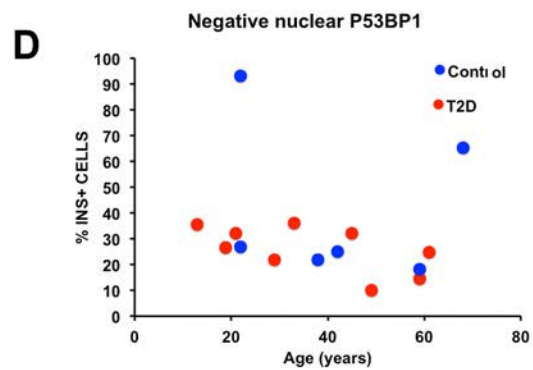

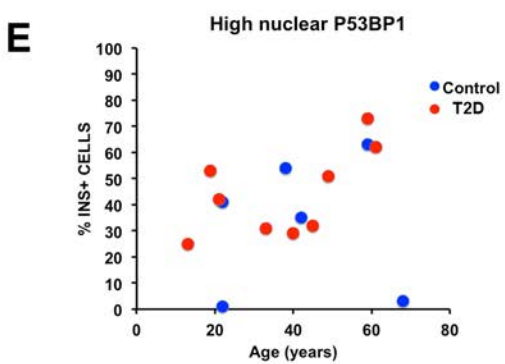

Suppl. Figure 6

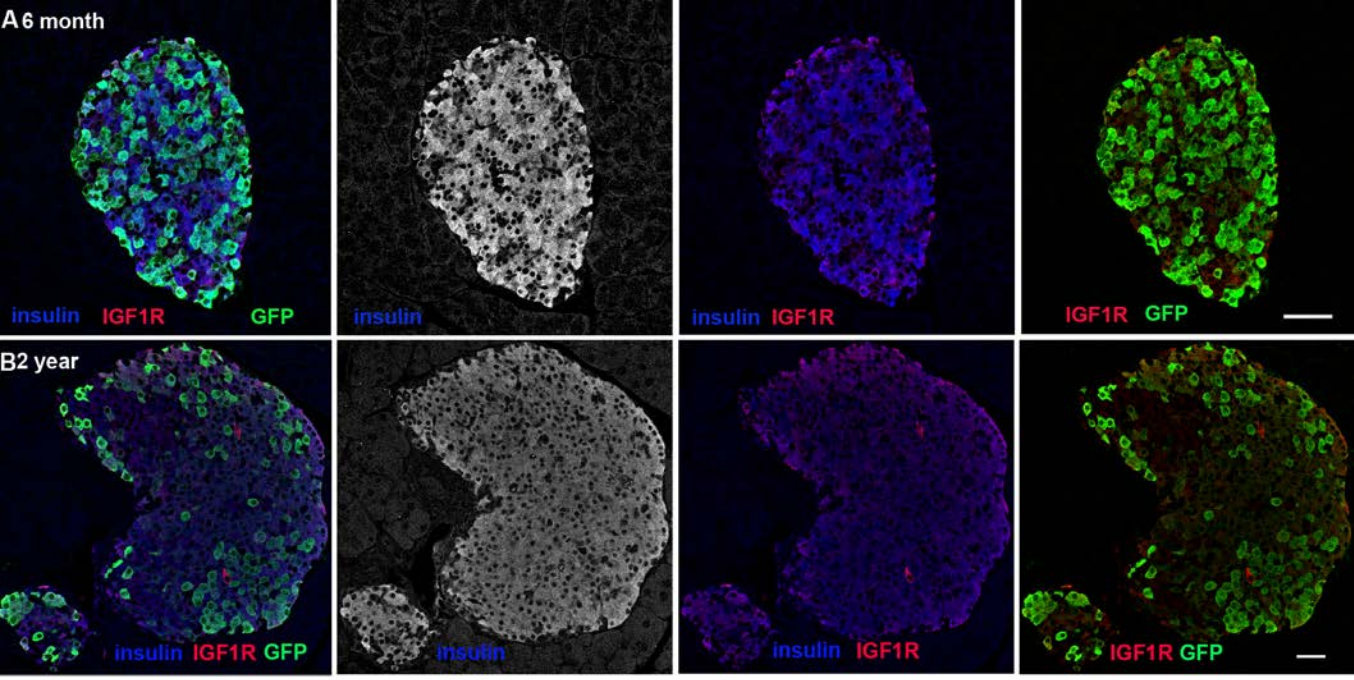

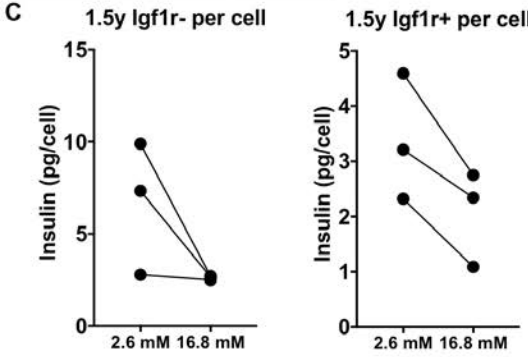

Suppl. Figure 7

SUPPLEMENTAL INFORMATION

Supplementary Figure 1. Changes of β-cell aging markers occur even in aged mice that remain normoglycemic. Related to Figures 1 and 3. INK-ATTAC mice at 1y show neither a decline in glucose tolerance after IPGGT (**A**) nor fasting hyperglycemia (**B**). Yet with age there is an increase in basal insulin secretion (**C**). Data presented for each of the triplicate samples (10 islets) of 7 individual mice/age. Additionally with age IGF1R protein levels increased (**D**) and KCNQ5 protein decreased (**E**). n=4 animals/age. **F**. Co-localization of IGF1R and p16 reporter FLAG in a subset of cells from 4-6 m INK-ATTAC mice. Data are Means ± SEM. Magnification bar=25 μm (D, E); 50 μm (F).

Supplementary Figure 2. Individual β-cell insulin secretion and β-cell FACS sorting criteria. Related to Figure 1 and STAR methods. In reverse hemolytic plaque assay (RHPA), the immunoplaque area is directly proportional to the amount of insulin secreted by individual β cells. Representative pictures of non-secreting (**A**), small plaques (**B**), medium plaques (**C**) or large plaques (**D**); this image has been previously published in (Aguayo-Mazzucato et al., 2011). Magnification bar= 100 μm Insulin secretion is comparable using static incubation (insulin pg/ngDNA) **(E**) or the reverse hemolytic plaque assay (secretion index=% secreting cells X plaque area) (**F**). **G**. FACS sorting criteria for a purified fraction of β cells based on autofluorescence (King et al., 2007). Data are Means ± SEM.

Supplementary Figure 3. Age-induced changes in β-cell and senescence gene sets. Related to Figure 2C. Heatmaps of gene expression from microarray data of purified β-cells from young, 1y and 2y old mice showing changes in expression of Hallmark β cell (A) and GO Cellular senescence (B) gene sets. Comparison of young to 1 y shows increased maturation of β-cell identity whereas comparison of 1y and 2 y show increase in cellular senescent genes. These data show that some characteristic β-cell genes are turned off with aging however, the overall gene expression profile is very different between

young and 2 year old supporting the presence of different phenotypes at different life stages of a β-cell.

Supplementary Figure 4. ***CD99*** **mRNA and protein timecourse. Related to Figure 2F.** Timecourse expression of *CD99* mRNA (**A**) and quantification of protein expression by densitometry(**B**). Same samples as used in Figure 2F and 3A. At 2m there are two subpopulations, a high and low; the low disappears with age. Data are Means ± SEM.

Supplementary Figure 5. Plasma membrane expression of aging markers. Related to Figure 3. IGF1R and KCNQ5 colocalize with cell membrane marker E-Cadherin. Plasma membrane staining of IGF1R is more clearly seen in ducts (D) and acinar cells, which have lower levels of cytoplasmic expression than β cells. Merged and then single channels shown. Magnification bar=10 μm

Supplementary Figure 6. Expression of β-cell aging markers in human β-cells and changes induced by T2D. Related to Figures 3F and 6. β-cells of human donors express higher levels of IGF1R protein with age (**A**) and with T2D (**B**) protein as seen by immunostaining. Magnification bar=50 μm **C**. The presence of T2D in young donors appears to induce P53BP1 and IGF1R expression. Quantification of β-cells that were negative (**D**) or highly positive (**E**) for nuclear P53BP1 in pancreas from donors with and without T2D over a range of ages. Details of the human donors are given in **Key Resources.** Data are values for individual donors.

Supplementary Figure 7. Expression of IGF1R in β-cells from MIP-GFP mice and insulin secretion from IGF1R positive and negative β-cells obtained from old mice. Related to Figures 3I and 4C. Representative pictures of insulin, IGF1R and GFP co-expression from 6 m (**A**) and 2 y (**B**) MIP:GFP mice showing the decline of GFP expression with age. Merged and separated channels. Magnification bar=50 μm. GFP antibody had been optimized to show differential

expression whereas that of insulin was not. Even GFP^{low} were stained for insulin. **C**. Both IGF1R+ and IGF1R- β-cells from 1.5 y C57Bl/6J mice lack glucose-stimulated insulin secretion. n=3 independent cell preparations. Data are Means ± SEM

Supplementary Table 1. Top 550 cells surface genes differentially expressed between young and aged β cells as shown in the volcano plot (**Related to Fig. 2D**).

REFERENCES FOR SUPPLEMENTAL INFORMATION

Aguayo-Mazzucato, C., Koh, A., El Khattabi, I., Li, W.C., Toschi, E., Jermendy, A., Juhl, K., Mao, K., Weir, G.C., Sharma, A., et al. (2011). Mafa expression enhances glucose-responsive insulin secretion in neonatal rat beta cells. Diabetologia *54*, 583-593.

King, A.J., Fernandes, J.R., Hollister-Lock, J., Nienaber, C.E., Bonner-Weir, S., and Weir, G.C. (2007). Normal relationship of beta- and non-beta-cells not needed for successful islet transplantation. Diabetes *56*, 2312-2318.